Optimization of composite structures

A topology and shape sensitivity analysis

Gabriel Delgado Keeffe
under the supervision of
Grégoire Allaire

Ecole Polytechnique
Airbus Group Innovations

11th June 2014

Main topics

1) Composite optimal design via a level-set method

2) Anisotropic topological derivative

Main topics

1) Composite optimal design via a level-set method

(a) Multi-layered composites

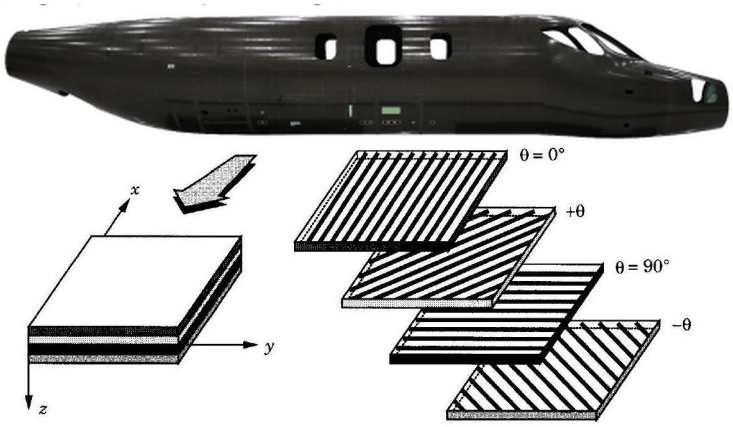

2) Anisotropic topological derivative

Main topics

1) Composite optimal design via a level-set method

(a) Multi-layered composites

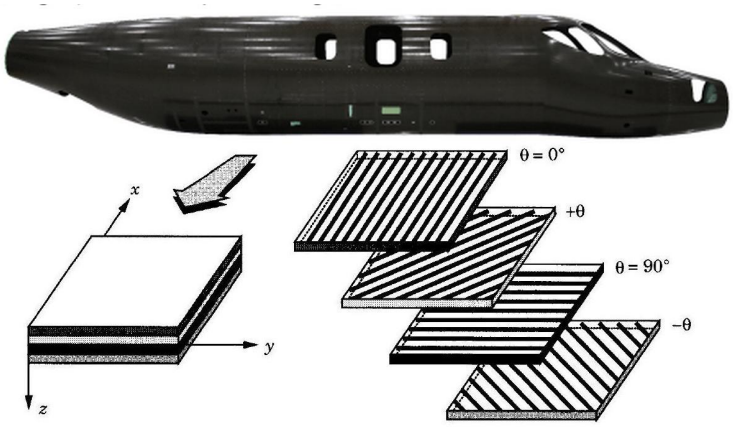

(b) Multi-phase materials

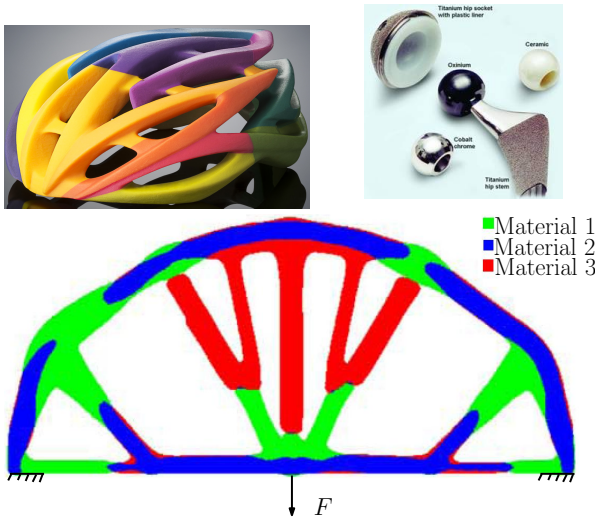

2) Anisotropic topological derivative

Main topics

1) Composite optimal design via a level-set method

(a) Multi-layered composites

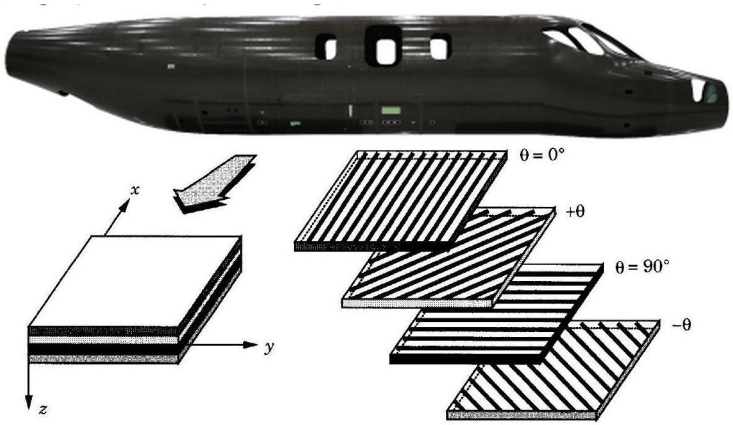

(b) Multi-phase materials

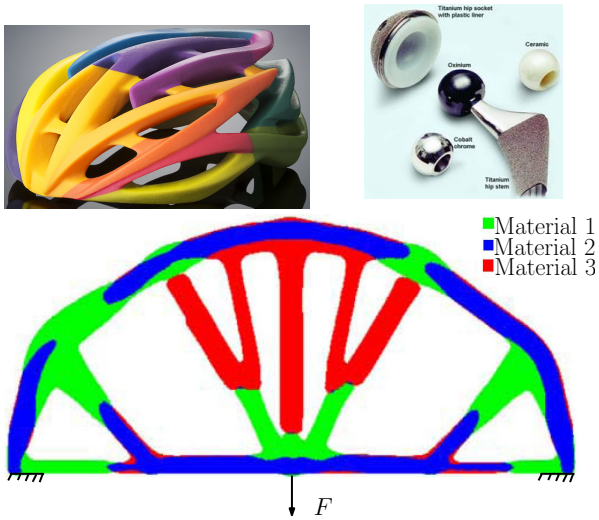

2) Anisotropic topological derivative

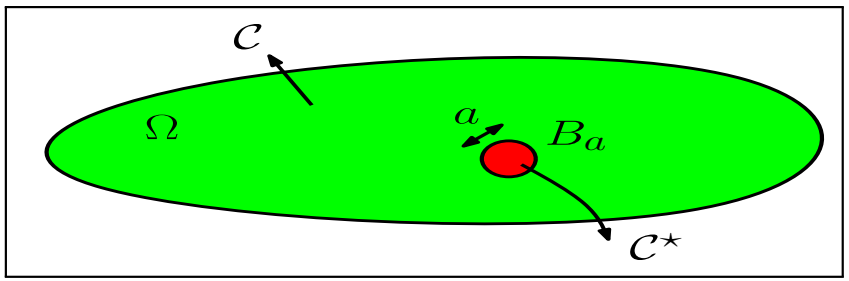

$$DJ = \lim_{a \to 0} \frac{J(a) - J(0)}{h(a)}$$

Main topics

1) Composite optimal design via a level-set method

(a) Multi-layered composites

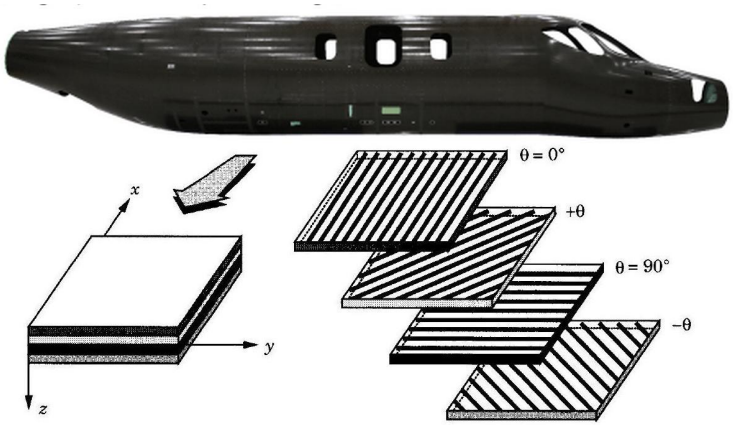

(b) Multi-phase materials

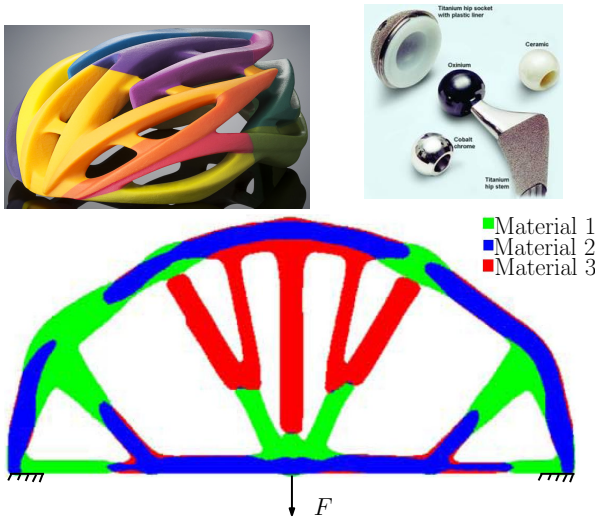

2) Anisotropic topological derivative

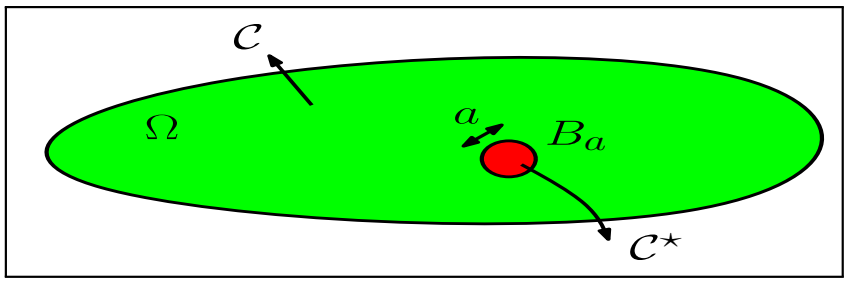

$$DJ = \lim_{a \to 0} \frac{J(a) - J(0)}{h(a)}$$

- Topology optimization.
- Inverse problems.

Outline

Outline

Topology optimization

A topology optimization problem can be cast as follows:

Find the stiffest structure $\omega \subset \Omega$ belonging to an admissible set $\mathcal{U}_{ad}$, which solves the problem

$$\min_{\omega \subset \Omega, \omega \in \mathcal{U}_{ad}} J(\omega, u(\omega)),$$

where $u(\omega)$ is the displacement field arising in ω due to prescribed excitations (f, g).

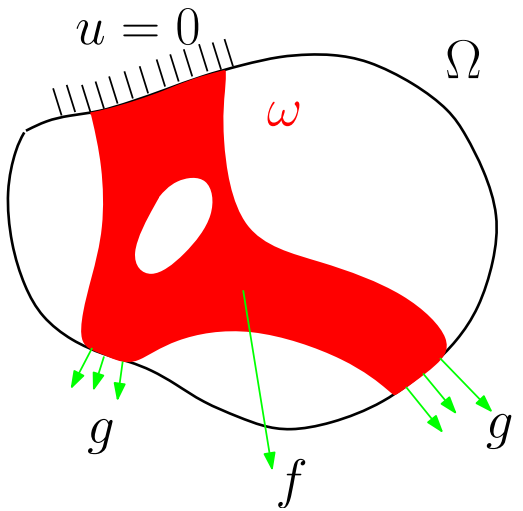

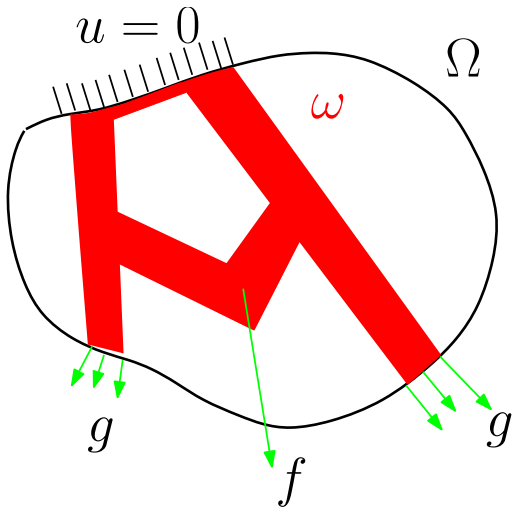

Topology optimization methods

Density based	Boundary variations
Homogenization [Murat and Tartar, 1985], [Bendsøe and Kikuchi, 1988]	Level set+Shape sensitivity analysis [Allaire et al., 2002], [Wang et al., 2003]
SIMP [Bendsøe, 1995]	Phase field [Chambolle and Bourdin, 2000]

Topology optimization methods

Density based	Boundary variations
Homogenization [Murat and Tartar, 1985], [Bendsøe and Kikuchi, 1988]	Level set+Shape sensitivity analysis [Allaire et al., 2002], [Wang et al., 2003]
SIMP [Bendsøe, 1995]	Phase field [Chambolle and Bourdin, 2000]

Characteristics

- No need of remeshing.
- Allows naturally topology changes.

Topology optimization methods

Density based	Boundary variations
Homogenization [Murat and Tartar, 1985], [Bendsøe and Kikuchi, 1988]	Level set+Shape sensitivity analysis [Allaire et al., 2002], [Wang et al., 2003]
SIMP [Bendsøe, 1995]	Phase field [Chambolle and Bourdin, 2000]

Characteristics

- No need of remeshing.
- Allows naturally topology changes.

Comparative advantages

- Clear contour of the shape.
- Easy definition of geometrical parameters.

The Level-set method

- Introduced by [Osher and Sethian, 1988].

The Level-set method

- Introduced by [Osher and Sethian, 1988].
- Definition of the level set function $\psi : \Omega \to \mathbb{R}$, with $\Omega \subset \mathbb{R}^d$ $(d = 2, 3)$

$$\begin{cases} \psi(x) = 0 \Leftrightarrow & x \in \partial\omega, \\ \psi(x) < 0 \Leftrightarrow & x \in \omega, \\ \psi(x) > 0 \Leftrightarrow & x \in \Omega\backslash\omega. \end{cases}$$

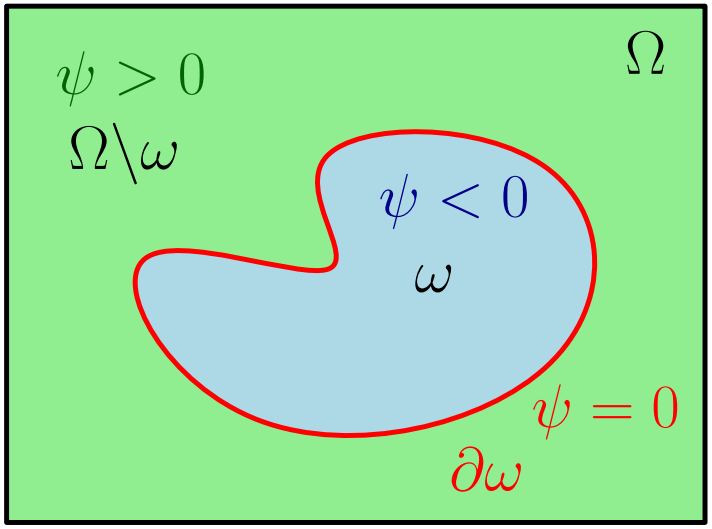

The Level-set method

- Introduced by [Osher and Sethian, 1988].
- Definition of the level set function $\psi : \Omega \to \mathbb{R}$, with $\Omega \subset \mathbb{R}^d$ $(d = 2, 3)$

$$\begin{cases} \psi(x) = 0 \Leftrightarrow & x \in \partial\omega, \\ \psi(x) < 0 \Leftrightarrow & x \in \omega, \\ \psi(x) > 0 \Leftrightarrow & x \in \Omega\backslash\omega. \end{cases}$$

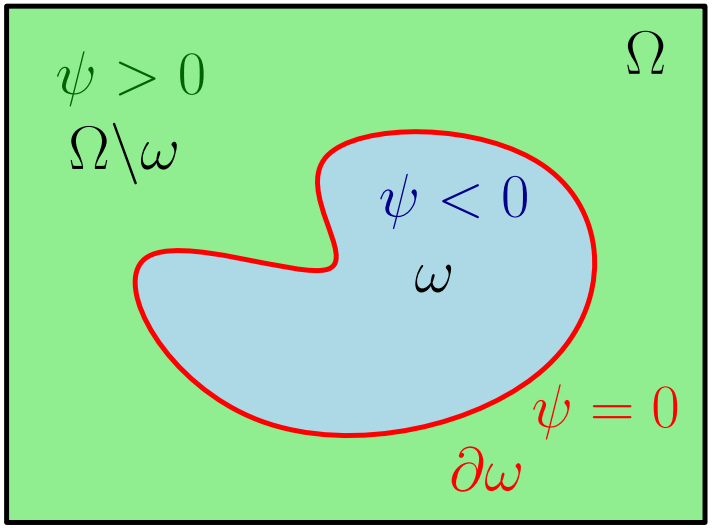

- Evolution of the shape $\omega(t), t \in \mathbb{R}$
  Level-set function $\psi(x, t)$

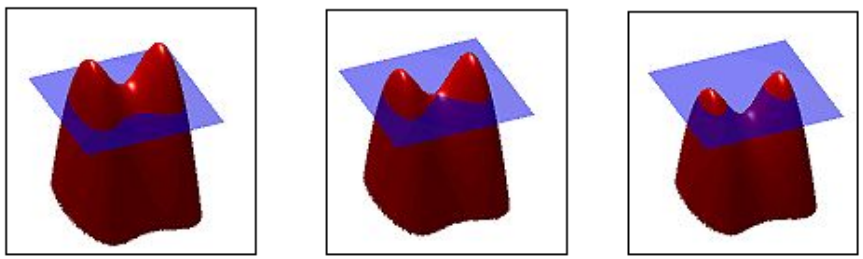

The Level-set method

- Introduced by [Osher and Sethian, 1988].
- Definition of the level set function $\psi : \Omega \to \mathbb{R}$, with $\Omega \subset \mathbb{R}^d$ $(d = 2, 3)$

$$\begin{cases} \psi(x) = 0 \Leftrightarrow & x \in \partial\omega, \\ \psi(x) < 0 \Leftrightarrow & x \in \omega, \\ \psi(x) > 0 \Leftrightarrow & x \in \Omega\backslash\omega. \end{cases}$$

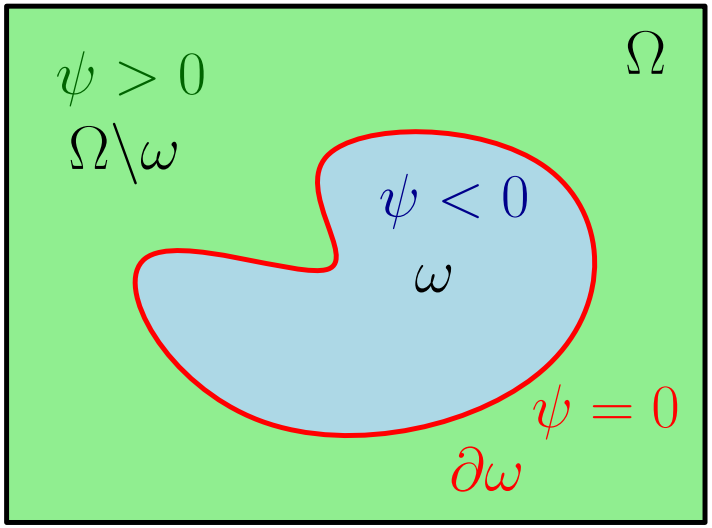

- Evolution of the shape $\omega(t), t \in \mathbb{R}$
  Level-set function $\psi(x, t)$

Shape $\omega(t)$

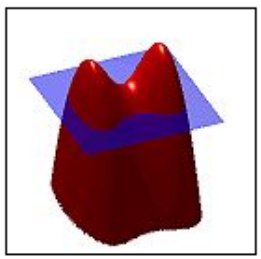
t_0

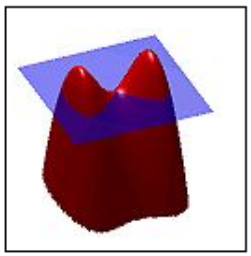
t_1

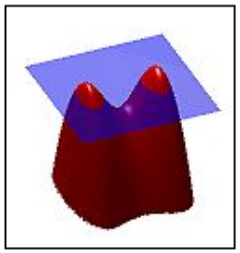
t_2

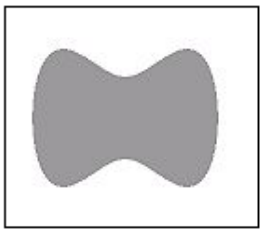
t_0

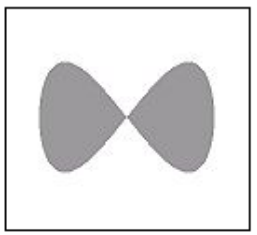
t_1

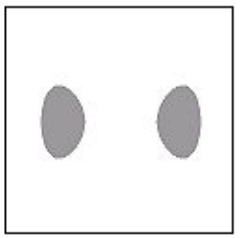
t_2

The Level-set method

- If the shape evolves according to a velocity field $\theta(x,t)$ defined on Ω with normal component $\mathcal{V}(x,t)$

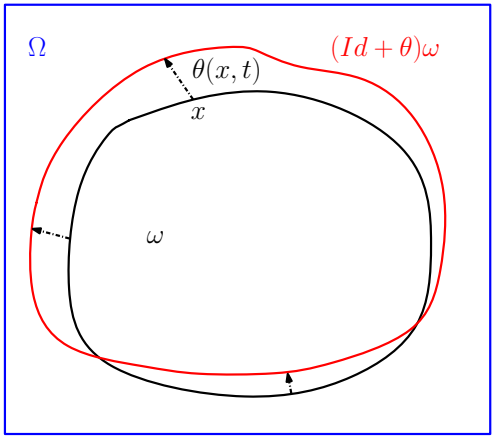

Figure: Deformation of ω

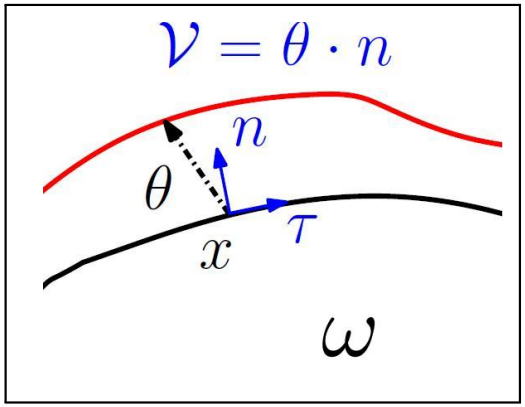

Figure: Zoom around x

The Level-set method

- If the shape evolves according to a velocity field $\theta(x,t)$ defined on Ω with normal component $\mathcal{V}(x,t)$

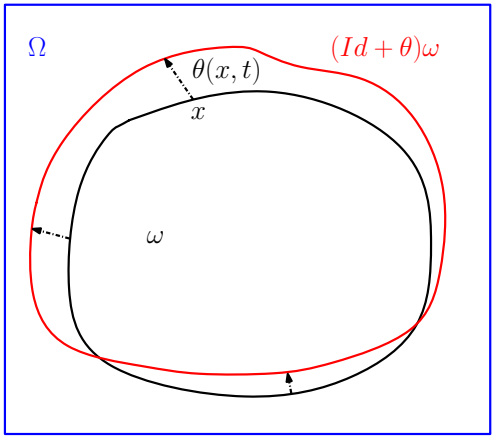

Figure: Deformation of ω

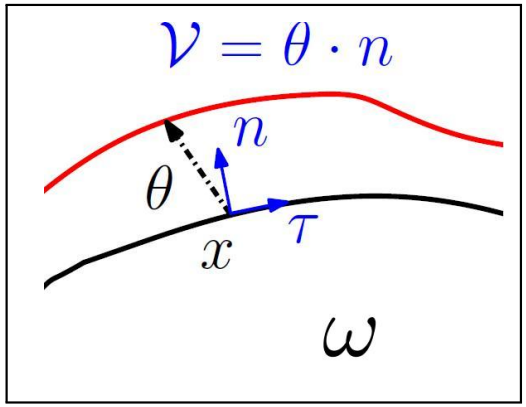

Figure: Zoom around x

- One can show that the evolution equation satisfied by ψ reads

$$\begin{cases} \dfrac{\partial\psi}{\partial t}+\mathcal{V}|\nabla\psi|=0 & x\in\Omega, t>0, \\ \psi=\psi_0 & x\in\Omega, t=0, \\ \dfrac{\partial\psi}{\partial n}=0 & x\in\partial\Omega, t>0. \end{cases}$$

Shape sensitivity analysis

Definition [Hadamard, 1908], [Simon and Murat, 1976]

Consider the following type of variations of $\omega \subset \Omega$

$$\big(Id + \theta\big)(\omega) := \{x + \theta(x) \text{ for } \ x \in \omega\}, \theta \in W^{1,\infty}(\Omega; \mathbb{R}^d)$$

The shape derivative of a function $J(\omega)$ is defined as the Fréchet derivative in $W^{1,\infty}(\Omega; \mathbb{R}^d)$ at 0 of the application $\theta \to J\big(\big(Id + \theta\big)\omega\big)$, i.e.

$$J\big(\big(Id + \theta\big)\omega\big) = J(\omega) + J'(\omega)(\theta) + o(\theta).$$

Shape sensitivity analysis

Definition [Hadamard, 1908], [Simon and Murat, 1976]

Consider the following type of variations of $\omega \subset \Omega$

$$\big(Id+\theta\big)(\omega) := \{x+\theta(x) \text{ for } \ x \in \omega\}, \theta \in W^{1,\infty}(\Omega;\mathbb{R}^d)$$

The shape derivative of a function $J(\omega)$ is defined as the Fréchet derivative in $W^{1,\infty}(\Omega;\mathbb{R}^d)$ at 0 of the application $\theta \to J\big(\big(Id+\theta\big)\omega\big)$, i.e.

$$J\big(\big(Id+\theta\big)\omega\big) = J(\omega) + J'(\omega)(\theta) + o(\theta).$$

Proposition

Suppose ω and J regular, then there exists a continuous linear form l such that

$$J'(\omega)(\theta) = l((\theta \cdot n)|_{\partial\omega})$$

Shape sensitivity analysis

Definition [Hadamard, 1908], [Simon and Murat, 1976]

Consider the following type of variations of $\omega \subset \Omega$

$$\big(Id+\theta\big)(\omega) := \{x+\theta(x) \text{ for } \ x \in \omega\}, \theta \in W^{1,\infty}(\Omega;\mathbb{R}^d)$$

The shape derivative of a function $J(\omega)$ is defined as the Fréchet derivative in $W^{1,\infty}(\Omega;\mathbb{R}^d)$ at 0 of the application $\theta \to J\big(\big(Id+\theta\big)\omega\big)$, i.e.

$$J\big(\big(Id+\theta\big)\omega\big) = J(\omega) + J'(\omega)(\theta) + o(\theta).$$

Proposition

Suppose ω and J regular, then there exists a continuous linear form l such that

$$J'(\omega)(\theta) = l((\theta \cdot n)|_{\partial\omega}) = \int_{\partial\omega} (\theta \cdot n) j ds$$

Coupling the level set method and shape derivative

- The objective is to find a normal descent direction $\mathcal{V}^*$ such that

$$\left\{ \begin{array}{lcl} \psi(t_0, \cdot) & \equiv & \omega \\ \psi(t_0 + \Delta t, \cdot) & \equiv & \omega^{\Delta t} \end{array} \right. \Rightarrow \quad J(\omega^{\Delta t}) - J(\omega) < 0$$

$$\frac{\partial \psi}{\partial t} + \mathcal{V}^* |\nabla \psi| = 0; \quad t \in [t_0, t_0 + \Delta t], x \in \Omega$$

Coupling the level set method and shape derivative

- The objective is to find a normal descent direction $\mathcal{V}^*$ such that

$$\left\{ \begin{array}{lcl} \psi(t_0, \cdot) & \equiv & \omega \\ \psi(t_0 + \Delta t, \cdot) & \equiv & \omega^{\Delta t} \end{array} \right. \Rightarrow \quad J(\omega^{\Delta t}) - J(\omega) < 0$$

$$\frac{\partial \psi}{\partial t} + \mathcal{V}^* |\nabla \psi| = 0; \quad t \in [t_0, t_0 + \Delta t], x \in \Omega$$

- This direction can be deduced from the solution of the variational problem

$$\langle \mathcal{V}^*, v \rangle_{H^1(\Omega)} = -l(v), \forall v \in H^1(\Omega),$$

Coupling the level set method and shape derivative

- The objective is to find a normal descent direction $\mathcal{V}^*$ such that

$$\left\{ \begin{array}{lcl} \psi(t_0, \cdot) & \equiv & \omega \\ \psi(t_0 + \Delta t, \cdot) & \equiv & \omega^{\Delta t} \end{array} \right. \Rightarrow \quad J(\omega^{\Delta t}) - J(\omega) < 0$$

$$\frac{\partial \psi}{\partial t} + \mathcal{V}^* |\nabla \psi| = 0; \quad t \in [t_0, t_0 + \Delta t], x \in \Omega$$

- This direction can be deduced from the solution of the variational problem

$$\langle \mathcal{V}^*, v \rangle_{H^1(\Omega)} = -l(v), \forall v \in H^1(\Omega),$$

Coupling the level set method and shape derivative

- The objective is to find a normal descent direction $\mathcal{V}^*$ such that

$$\left\{ \begin{array}{lcl} \psi(t_0, \cdot) & \equiv & \omega \\ \psi(t_0 + \Delta t, \cdot) & \equiv & \omega^{\Delta t} \end{array} \right. \Rightarrow \quad J(\omega^{\Delta t}) - J(\omega) < 0$$

$$\frac{\partial \psi}{\partial t} + \mathcal{V}^* |\nabla \psi| = 0; \quad t \in [t_0, t_0 + \Delta t], x \in \Omega$$

- This direction can be deduced from the solution of the variational problem

$$\langle \mathcal{V}^*, v \rangle_{H^1(\Omega)} = -l(v), \forall v \in H^1(\Omega), \quad l(v) = J'(\omega)(vn),$$

Coupling the level set method and shape derivative

- The objective is to find a normal descent direction $\mathcal{V}^*$ such that

$$\left\{\begin{array}{lcl}\psi(t_0,\cdot) & \equiv & \omega \\ \psi(t_0+\Delta t,\cdot) & \equiv & \omega^{\Delta t}\end{array}\right. \Rightarrow \quad J(\omega^{\Delta t}) - J(\omega) < 0$$

$$\frac{\partial \psi}{\partial t} + \mathcal{V}^* |\nabla \psi| = 0; \quad t \in [t_0, t_0+\Delta t], x \in \Omega$$

- This direction can be deduced from the solution of the variational problem

$$\langle \mathcal{V}^*, v \rangle_{H^1(\Omega)} = -l(v), \forall v \in H^1(\Omega), \quad l(v) = J'(\omega)(vn),$$

Indeed, for Δt small enough

$$\begin{array}{rcl} J(\omega^{\Delta t}) - J(\omega) & = & \Delta t \times J'(\omega)(\theta^*) + o(\Delta t), \quad \theta^* = \mathcal{V}^* n \\ & = & \Delta t \times l(\mathcal{V}^*) + o(\Delta t) \\ & = & -\Delta t \times \|\mathcal{V}^*\|^2_{H^1(\Omega)} + o(\Delta t) < 0 \end{array}$$

The level set method for topology optimization

- Optimization of a triangular car suspension (courtesy of G. Allaire).

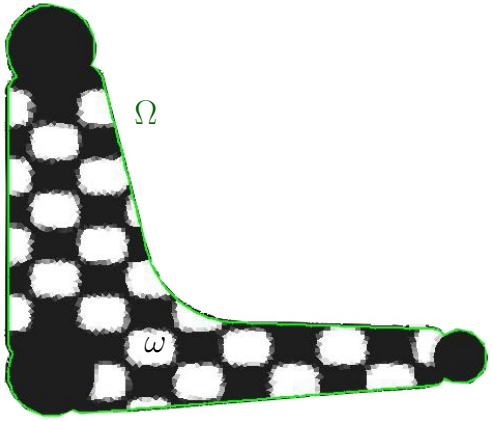

Figure: Iteration 1

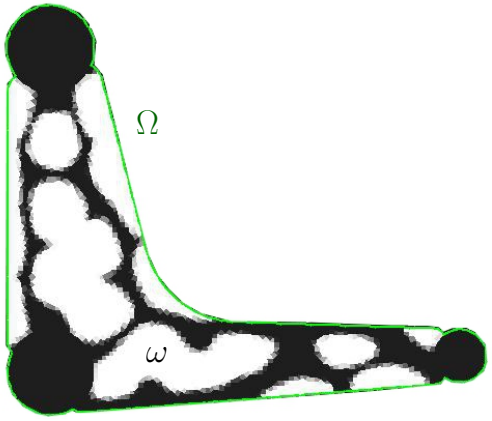

Figure: Iteration 26

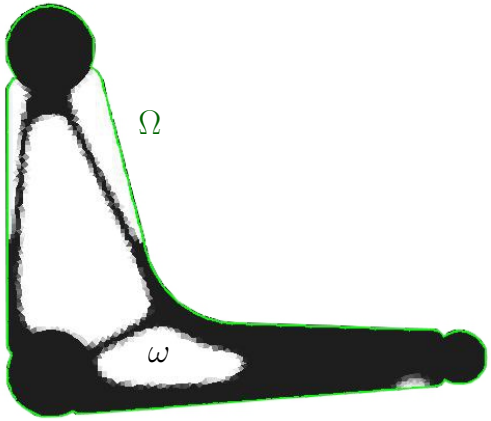

Figure: Iteration 100

Linear elasticity:

$$\begin{cases} -\text{div}(Ce(u)) = 0 & \text{in } \Omega \\ u = 0 & \text{on } \Gamma_D \\ Ce(u)\cdot n = g & \text{on } \Gamma_N \end{cases}$$

$$\min_{\omega\subset\Omega,|\omega|=c} J(\omega), \quad J(\omega) = \int_{\Gamma_N} g\cdot u ds$$

$$J'(\omega)(\theta) = -\int_{\partial\omega} \theta\cdot n(Ce(u) : e(u))dx$$

Outline

Multi-phase optimal design

- Design variable: shape of each phase (n level-sets $\rightarrow 2^n$ materials)

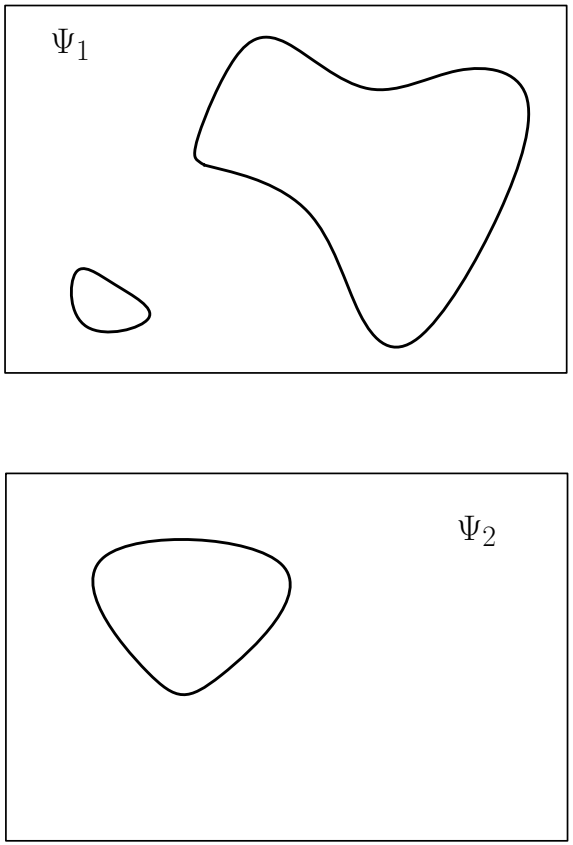

Figure: Level-set functions Ψ_1, Ψ_2

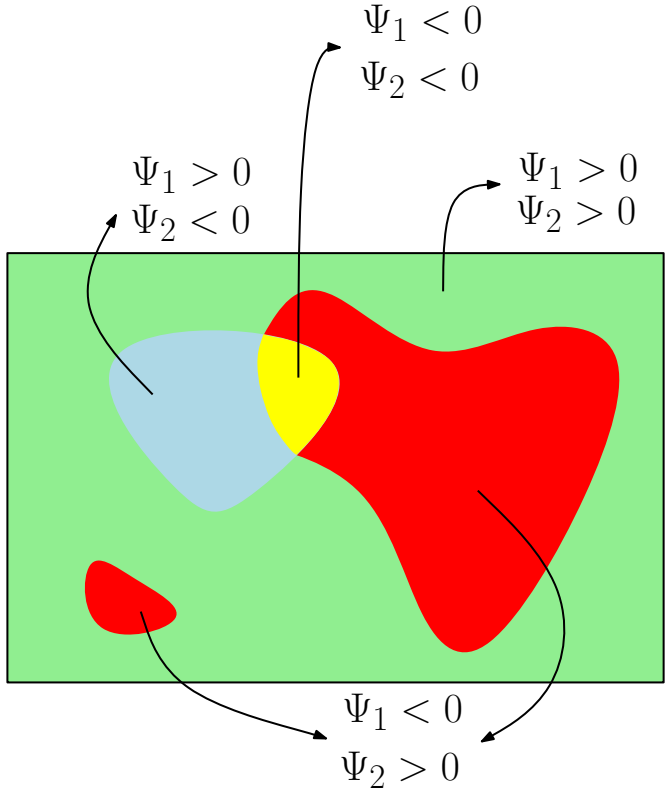

Figure: Multi-phase material via superposition of Ψ_1, Ψ_2

Multi-layered optimal design

- Design variables: shape of each ply Ψ_i (continuous) & stacking sequence ξ (discrete)

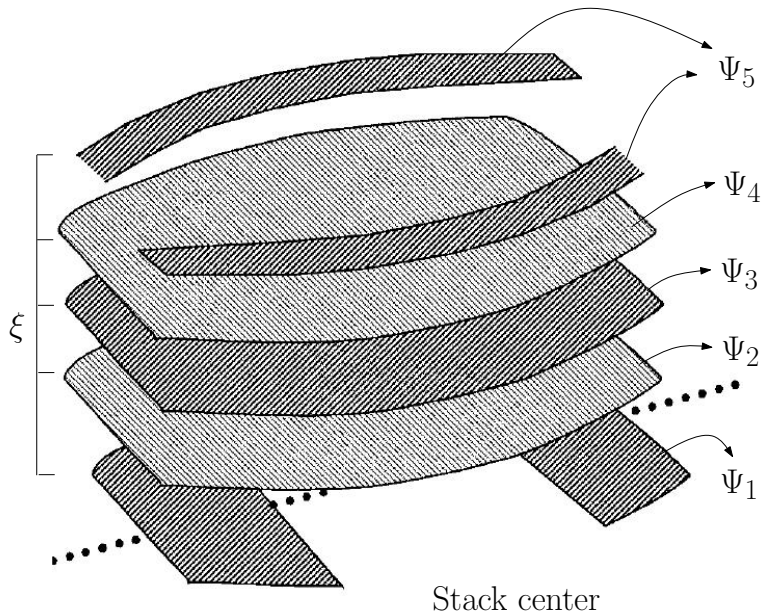

Figure: Multi-layered configuration

Multi-layered optimal design

- Design variables: shape of each ply Ψ_i (continuous) & stacking sequence ξ (discrete)

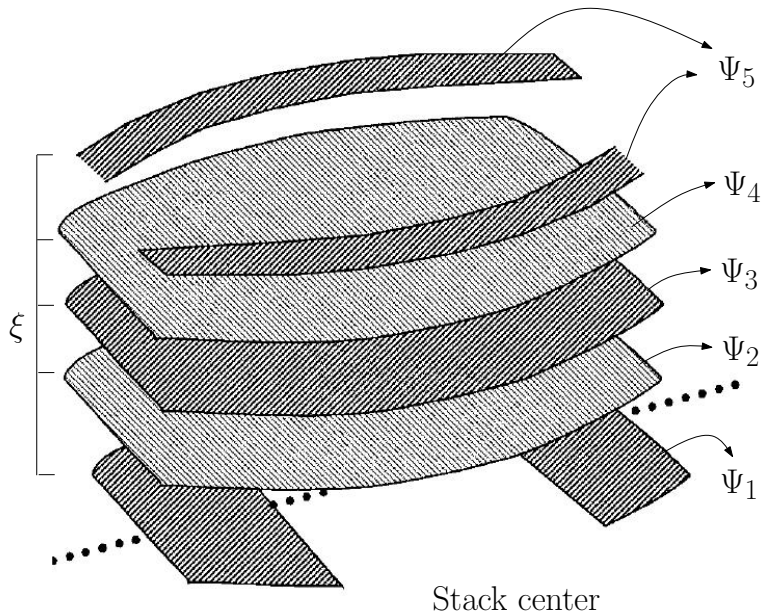

Figure: Multi-layered configuration

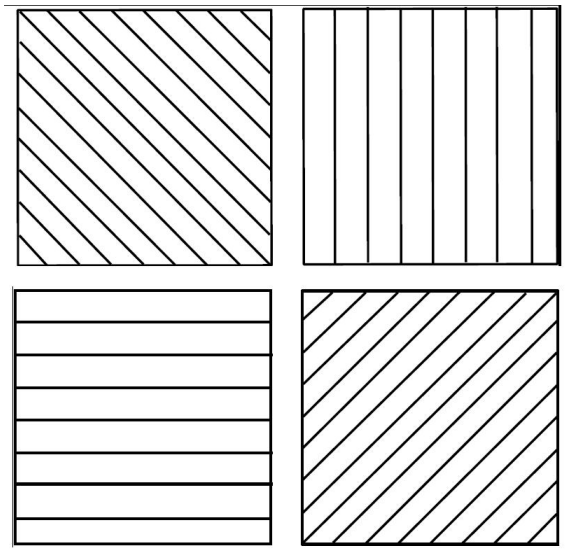

Figure: Orthotropic plies. Reinforced fibers in orientations $-45^o, 90^o, 0^o, 45^o$

The buckling problem

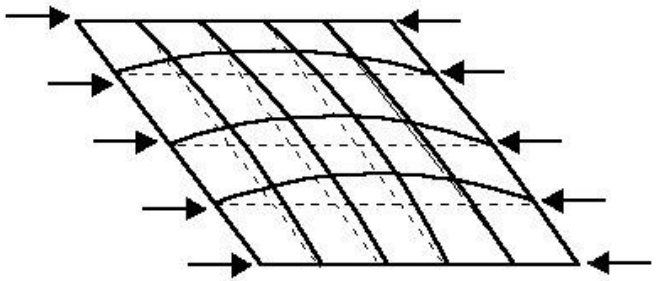

Figure: Buckling under compression

Figure: Buckled wing

The buckling problem

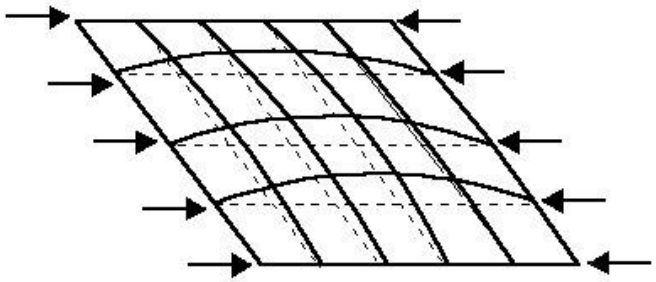

Figure: Buckling under compression

Figure: Buckled wing

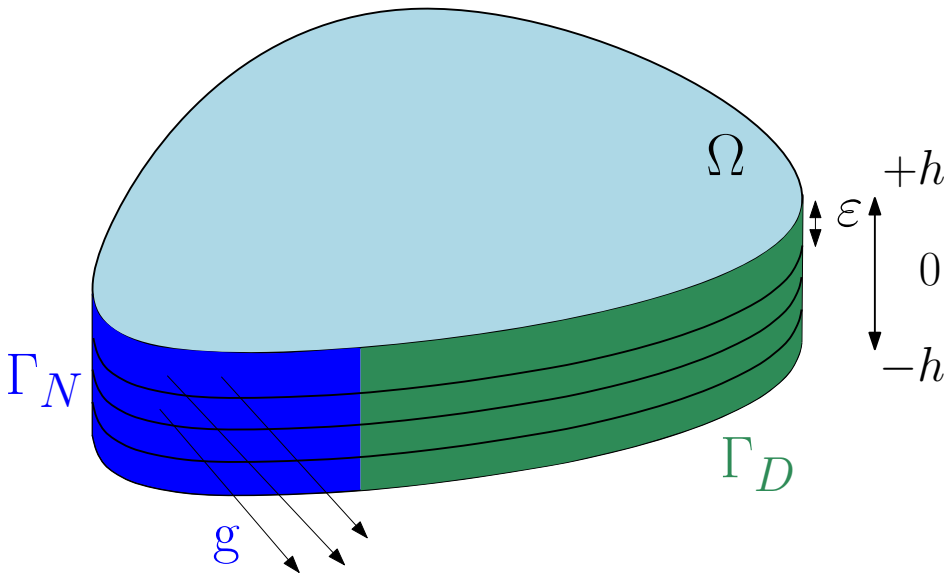

- Ω : Hold-all domain
- g : in-plane loads
- Γ_N : Neumann BC
- Γ_D : Dirichlet BC
- ε : Thickness of each ply
- $2h$: Total thickness laminate
- $\mathcal{A}$: extensional stiffness
- $\mathcal{D}$: bending stiffness

The buckling problem

$$\mathcal{A} = 2\varepsilon \sum_{i=1}^{N} \Big(\chi^i \mathcal{A}^i + (1-\chi^i)\mathcal{A}^0 \Big), \quad \chi^i : \text{ characteristic function}$$

$$\mathcal{D} = \frac{2\varepsilon^3}{3} \sum_{i=1}^{N} \Big(i^3 - (i-1)^3 \Big) \Big(\chi^i \mathcal{A}^i + (1-\chi^i)\mathcal{A}^0 \Big)$$

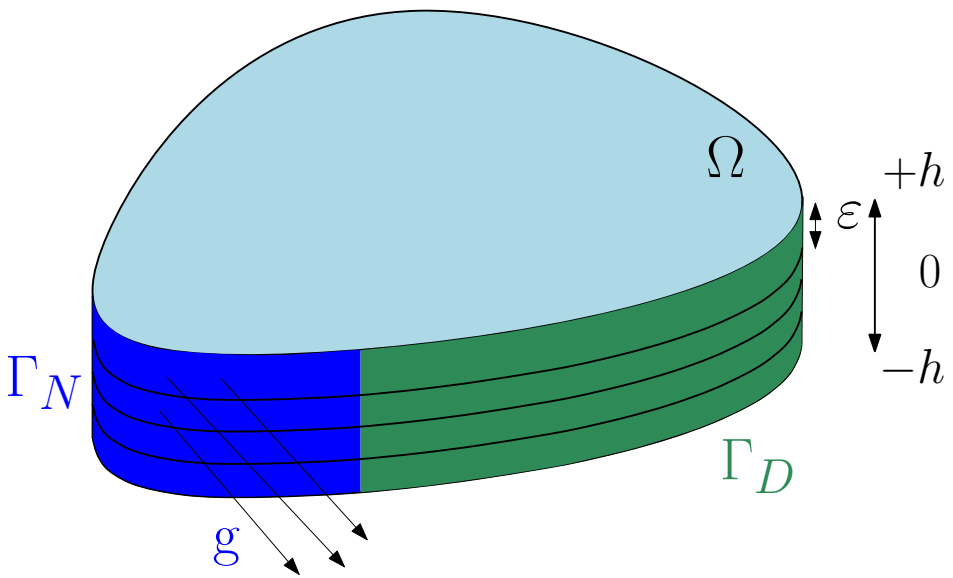

- Ω : Hold-all domain
- g : in-plane loads
- Γ_N : Neumann BC
- Γ_D : Dirichlet BC
- ε : Thickness of each ply
- $2h$: Total thickness laminate
- $\mathcal{A}$: extensional stiffness
- $\mathcal{D}$: bending stiffness

The buckling problem

$$\mathcal{A} = 2\varepsilon \sum_{i=1}^{N} \Big(\chi^i \mathcal{A}^i + (1-\chi^i)\mathcal{A}^0 \Big), \quad \chi^i : \text{ characteristic function}$$

$$\mathcal{D} = \frac{2\varepsilon^3}{3} \sum_{i=1}^{N} \Big(i^3 - (i-1)^3 \Big) \Big(\chi^i \mathcal{A}^i + (1-\chi^i)\mathcal{A}^0 \Big)$$

The multi-layered design problem becomes a multi-phase design problem.

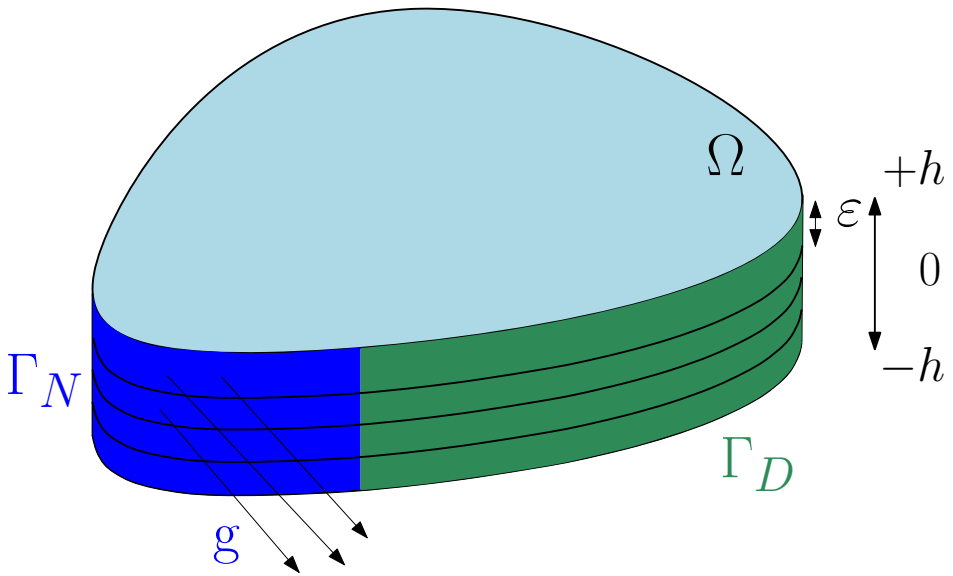

- Ω : Hold-all domain
- g : in-plane loads
- Γ_N : Neumann BC
- Γ_D : Dirichlet BC
- ε : Thickness of each ply
- $2h$: Total thickness laminate
- $\mathcal{A}$: extensional stiffness
- $\mathcal{D}$: bending stiffness

The linearized buckling problem

Definition (von Kármán plate model)

Let $u \in H^1(\Omega;\mathbb{R}^2)$ be the in-plane displacement and solves

$$\begin{cases} -\mathrm{div}(\mathcal{A}e(u)) = 0 & \text{in } \Omega, \\ u = 0 & \text{on } \Gamma_D, \\ \mathcal{A}e(u)\cdot n = 2hg, & \text{on } \Gamma_N. \end{cases}$$

The linearized buckling problem

Definition (von Kármán plate model)

Let $w \in H^2(\Omega)$ be the vertical displacement. Consider the eigenvalue problem

$$\begin{cases} \nabla^2 : (\mathcal{D}\nabla^2 w) = \lambda \mathcal{A}e(u) : \nabla^2 w & \text{in } \Omega, \end{cases}$$

Let $u \in H^1(\Omega; \mathbb{R}^2)$ be the in-plane displacement and solves

$$\begin{cases} -\mathrm{div}(\mathcal{A}e(u)) = 0 & \text{in } \Omega, \\ u = 0 & \text{on } \Gamma_D, \\ \mathcal{A}e(u) \cdot n = 2hg, & \text{on } \Gamma_N. \end{cases}$$

The linearized buckling problem

Definition (von Kármán plate model)

Let $w \in H^2(\Omega)$ be the vertical displacement. Consider the eigenvalue problem

$$\begin{cases} \nabla^2 : (\mathcal{D}\nabla^2 w) = \lambda \mathcal{A}e(u) : \nabla^2 w & \text{in } \Omega, \end{cases}$$

Let $u \in H^1(\Omega; \mathbb{R}^2)$ be the in-plane displacement and solves

$$\begin{cases} -\mathrm{div}(\mathcal{A}e(u)) = 0 & \text{in } \Omega, \\ u = 0 & \text{on } \Gamma_D, \\ \mathcal{A}e(u) \cdot n = 2hg, & \text{on } \Gamma_N. \end{cases}$$

We chose $\lambda = \lambda_1$, the smallest positive eigenvalue, as the critical buckling load.

The linearized buckling problem

Definition (von Kármán plate model)

Let $w \in H^2(\Omega)$ be the vertical displacement. Consider the eigenvalue problem

$$\begin{cases} \nabla^2 : (\mathcal{D}\nabla^2 w) = \lambda \mathcal{A}e(u) : \nabla^2 w & \text{in } \Omega, \\ w = 0, \nabla w \cdot n = 0 & \text{on } \Gamma_D, \end{cases}$$

Let $u \in H^1(\Omega; \mathbb{R}^2)$ be the in-plane displacement and solves

$$\begin{cases} -\mathrm{div}(\mathcal{A}e(u)) = 0 & \text{in } \Omega, \\ u = 0 & \text{on } \Gamma_D, \\ \mathcal{A}e(u) \cdot n = 2hg, & \text{on } \Gamma_N. \end{cases}$$

We chose $\lambda = \lambda_1$, the smallest positive eigenvalue, as the critical buckling load.

The linearized buckling problem

Definition (von Kármán plate model)

Let $w \in H^2(\Omega)$ be the vertical displacement. Consider the eigenvalue problem

$$\begin{cases} \nabla^2 : (\mathcal{D}\nabla^2 w) = \lambda \mathcal{A}e(u) : \nabla^2 w & \text{in } \Omega, \\ w = 0, \nabla w \cdot n = 0 & \text{on } \Gamma_D, \\ (\mathcal{D}\nabla^2 w)_{nn} = 0 & \text{on } \Gamma_N, \\ \nabla \cdot (\mathcal{D}\nabla^2 w) \cdot n + \frac{\partial}{\partial \tau}(\mathcal{D}\nabla^2 w)_{n\tau} = \lambda 2hg \cdot \nabla w & \text{on } \Gamma_N, \end{cases}$$

Let $u \in H^1(\Omega; \mathbb{R}^2)$ be the in-plane displacement and solves

$$\begin{cases} -\mathrm{div}(\mathcal{A}e(u)) = 0 & \text{in } \Omega, \\ u = 0 & \text{on } \Gamma_D, \\ \mathcal{A}e(u) \cdot n = 2hg, & \text{on } \Gamma_N. \end{cases}$$

We chose $\lambda = \lambda_1$, the smallest positive eigenvalue, as the critical buckling load.

Elastic transmission conditions (ETC)

Sharp interface formulation

$$\mathcal{A} = \mathcal{A}^1 + H(\psi)(\mathcal{A}^0 - \mathcal{A}^1)$$

$$\begin{cases} \mathcal{A}^1, \mathcal{A}^0 : \text{ Elastic phases} \\ H : \text{ Heaviside function.} \end{cases}$$

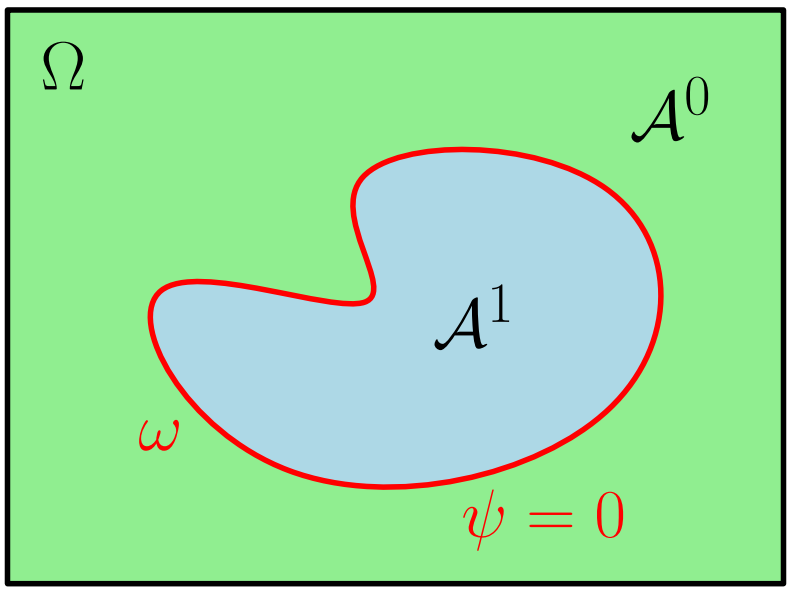

Elastic transmission conditions (ETC)

Sharp interface formulation

$$\mathcal{A} = \mathcal{A}^1 + H(\psi)(\mathcal{A}^0 - \mathcal{A}^1)$$

$$\begin{cases} \mathcal{A}^1, \mathcal{A}^0 : \text{ Elastic phases} \\ H : \text{ Heaviside function.} \end{cases}$$

Transmission conditions on $\psi = 0$ ($[\![\cdot]\!]$ denotes the jump through $\partial\omega$):

Elastic transmission conditions (ETC)

Sharp interface formulation

$$\mathcal{A} = \mathcal{A}^1 + H(\psi)(\mathcal{A}^0 - \mathcal{A}^1)$$

$$\begin{cases} \mathcal{A}^1, \mathcal{A}^0 : \text{ Elastic phases} \\ H : \text{ Heaviside function.} \end{cases}$$

Transmission conditions on $\psi = 0$ ($[\![\cdot]\!]$ denotes the jump through $\partial\omega$):

$$\begin{cases} [\![w]\!] = 0, \quad [\![\nabla w \cdot n]\!] = 0, \\ [\![(\mathcal{D}\nabla^2 w)_{nn}]\!] = 0, \\ [\![-\lambda_1(\mathcal{A}e(u) : \nabla w) \cdot n + \mathrm{div}(\mathcal{D}\nabla^2 w) \cdot n + \frac{\partial}{\partial \tau}(\mathcal{D}\nabla^2 w)_{n\tau}]\!] = 0 \end{cases} \qquad \begin{cases} [\![u]\!] = 0, \quad [\![\mathcal{A}e(u) \cdot n]\!] = 0 \end{cases}$$

Elastic transmission conditions (ETC)

Sharp interface formulation

$$\mathcal{A} = \mathcal{A}^1 + H(\psi)(\mathcal{A}^0 - \mathcal{A}^1)$$

$$\begin{cases} \mathcal{A}^1, \mathcal{A}^0 : \text{ Elastic phases} \\ H : \text{ Heaviside function.} \end{cases}$$

Transmission conditions on $\psi = 0$ ($[\![\cdot]\!]$ denotes the jump through $\partial\omega$):

$$\begin{cases} [\![w]\!] = 0, \quad [\![\nabla w \cdot n]\!] = 0, \\ [\![(\mathcal{D}\nabla^2 w)_{nn}]\!] = 0, \\ [\![-\lambda_1(\mathcal{A}e(u) : \nabla w) \cdot n + \mathrm{div}(\mathcal{D}\nabla^2 w) \cdot n + \frac{\partial}{\partial \tau}(\mathcal{D}\nabla^2 w)_{n\tau}]\!] = 0 \end{cases} \qquad \begin{cases} [\![u]\!] = 0, \quad [\![\mathcal{A}e(u) \cdot n]\!] = 0 \end{cases}$$

Elastic transmission conditions (ETC)

Sharp interface formulation

$$\mathcal{A} = \mathcal{A}^1 + H(\psi)(\mathcal{A}^0 - \mathcal{A}^1)$$

$$\begin{cases} \mathcal{A}^1, \mathcal{A}^0 : \text{ Elastic phases} \\ H : \text{ Heaviside function.} \end{cases}$$

Smooth interface formulation

$$\mathcal{A} = \mathcal{A}^1 + H_\epsilon(d_\omega)(\mathcal{A}^0 - \mathcal{A}^1)$$

$$\begin{cases} H_\epsilon : \text{ Regular approximation } H \\ \epsilon : \text{ Interpolation width.} \end{cases}$$

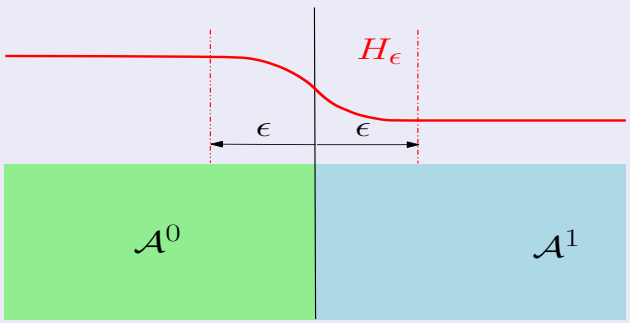

Elastic transmission conditions (ETC)

Sharp interface formulation

$$\mathcal{A} = \mathcal{A}^1 + H(\psi)(\mathcal{A}^0 - \mathcal{A}^1)$$

$$\begin{cases} \mathcal{A}^1, \mathcal{A}^0 : \text{ Elastic phases} \\ H : \text{ Heaviside function.} \end{cases}$$

Smooth interface formulation

$$\mathcal{A} = \mathcal{A}^1 + H_\epsilon(d_\omega)(\mathcal{A}^0 - \mathcal{A}^1)$$

$$\begin{cases} H_\epsilon : \text{ Regular approximation } H \\ \epsilon : \text{ Interpolation width.} \end{cases}$$

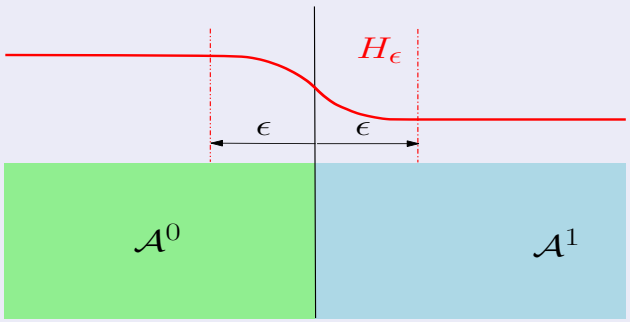

Signed distance function:

$$d_\omega(x) = \begin{cases} -d(x, \partial\omega) & \text{if } x \in \omega, \\ 0 & \text{if } x \in \partial\omega, \\ d(x, \partial\omega) & \text{if } x \in \Omega \backslash \bar{\omega}, \end{cases}$$

Composite optimization problem

Definition (Lightweight design problem)

Find the best composite structure $(\mathcal{O}, \xi)$, with:

Composite optimization problem

Definition (Lightweight design problem)

Find the best composite structure $(\mathcal{O}, \xi)$, with:

Collection of ply-shapes: $\mathcal{O} = \{\omega_i\}_{i=1\ldots N}$ Stacking sequence: ξ

Composite optimization problem

Definition (Lightweight design problem)

Find the best composite structure $(\mathcal{O}, \xi)$, with:

Collection of ply-shapes: $\mathcal{O} = \{\omega_i\}_{i=1\ldots N}$ Stacking sequence: ξ

$$\min_{\mathcal{O}\in\,\mathcal{U}_{ad},\xi\in Y} \{V(\mathcal{O})|G(\mathcal{O},\xi) \leq 0\}, \quad \text{where:}$$

Composite optimization problem

Definition (Lightweight design problem)

Find the best composite structure $(\mathcal{O}, \xi)$, with:

Collection of ply-shapes: $\mathcal{O} = \{\omega_i\}_{i=1\ldots N}$ Stacking sequence: ξ

$$\min_{\mathcal{O}\in\,\mathcal{U}_{ad},\xi\in Y} \{V(\mathcal{O})|G(\mathcal{O},\xi) \leq 0\}, \quad \text{where:}$$

Total weight: $V(\mathcal{O})$ Failure constraint: $G(\mathcal{O}, \xi)$

Composite optimization problem

Definition (Lightweight design problem)

Find the best composite structure $(\mathcal{O}, \xi)$, with:

Collection of ply-shapes: $\mathcal{O} = \{\omega_i\}_{i=1\dots N}$ Stacking sequence: ξ

$$\min_{\mathcal{O}\in\,\mathcal{U}_{ad},\xi\in Y} \{V(\mathcal{O}) | G(\mathcal{O},\xi) \leq 0\}, \quad \text{where:}$$

Total weight: $V(\mathcal{O})$
Admissible shapes: $\mathcal{U}_{ad}$

Failure constraint: $G(\mathcal{O},\xi)$
Admissible stacking: Y

Composite optimization problem

Definition (Lightweight design problem)

Find the best composite structure $(\mathcal{O}, \xi)$, with:

Collection of ply-shapes: $\mathcal{O} = \{\omega_i\}_{i=1\dots N}$ Stacking sequence: ξ

$$\min_{\mathcal{O}\in\,\mathcal{U}_{ad}, \xi\in Y} \{V(\mathcal{O}) | G(\mathcal{O}, \xi) \leq 0\}, \quad \text{where:}$$

Total weight: $V(\mathcal{O})$
Admissible shapes: $\mathcal{U}_{ad}$

Failure constraint: $G(\mathcal{O}, \xi)$
Admissible stacking: Y

Related works:

- Stacking sequence optimization: Gürdal, Haftka & co-workers (90's-)
- Fiber orientation tailoring: Lund & co-workers (2005-).

Composite optimization problem

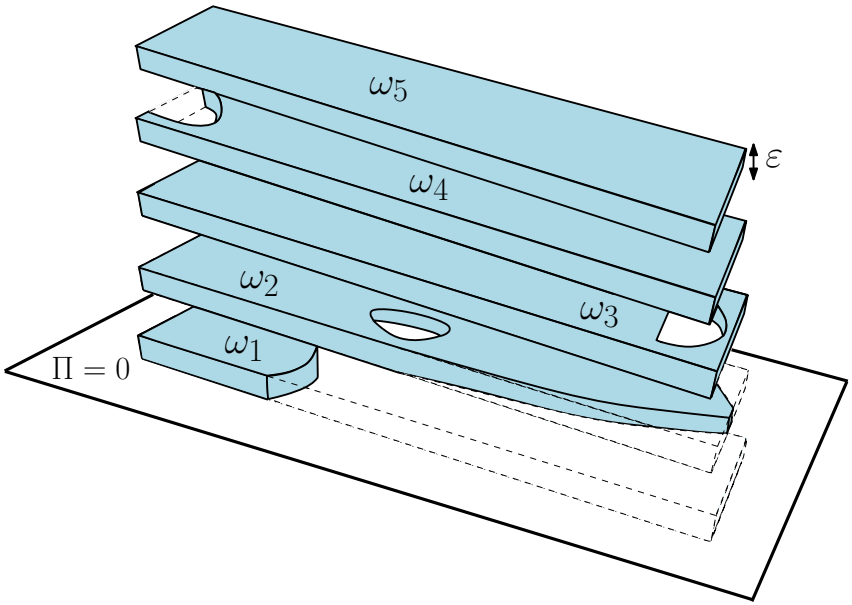

Figure: Each ply has its own shape ω_i

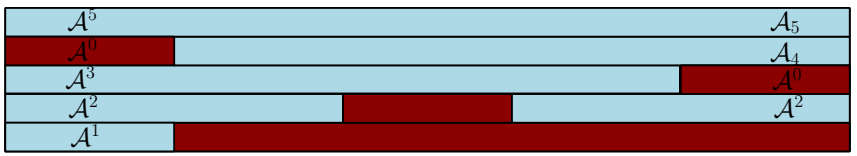

Figure: Transversal cut. Multi-phase structure.

Related works:

- Stacking sequence optimization: Gürdal, Haftka & co-workers (90's-)
- Fiber orientation tailoring: Lund & co-workers (2005-).

Bi-level formulation

Proposition

The mixed lightweight design composite problem can be equivalently written as

$$\min_{\mathcal{O}\in\mathcal{U}_{ad}} \{V(\mathcal{O})|\mathcal{M}(\mathcal{O}) \leq 0\},$$

where $\mathcal{M}$ constraint margin function $\mathcal{M}(\mathcal{O}) := \min_{\xi\in Y} G(\mathcal{O},\xi)$.

Bi-level formulation

Proposition

The mixed lightweight design composite problem can be equivalently written as

$$\min_{\mathcal{O}\in\mathcal{U}_{ad}} \{V(\mathcal{O})|\mathcal{M}(\mathcal{O}) \leq 0\},$$

where $\mathcal{M}$ constraint margin function $\mathcal{M}(\mathcal{O}) := \min_{\xi\in Y} G(\mathcal{O}, \xi)$.

Optimization algorithm

Let $\mathcal{O}^0 \in \mathcal{U}_{ad}$ be an initial feasible point. For $k \geq 0$, iterate until convergence

Bi-level formulation

Proposition

The mixed lightweight design composite problem can be equivalently written as

$$\min_{\mathcal{O}\in\mathcal{U}_{ad}} \{V(\mathcal{O})|\mathcal{M}(\mathcal{O}) \leq 0\},$$

where $\mathcal{M}$ constraint margin function $\mathcal{M}(\mathcal{O}) := \min_{\xi\in Y} G(\mathcal{O},\xi)$.

Optimization algorithm

Let $\mathcal{O}^0 \in \mathcal{U}_{ad}$ be an initial feasible point. For $k \geq 0$, iterate until convergence

$$\begin{cases}$$

Bi-level formulation

Proposition

The mixed lightweight design composite problem can be equivalently written as

$$\min_{\mathcal{O}\in\mathcal{U}_{ad}} \{V(\mathcal{O})|\mathcal{M}(\mathcal{O}) \leq 0\},$$

where $\mathcal{M}$ constraint margin function $\mathcal{M}(\mathcal{O}) := \min_{\xi\in Y} G(\mathcal{O},\xi)$.

Optimization algorithm

Let $\mathcal{O}^0 \in \mathcal{U}_{ad}$ be an initial feasible point. For $k \geq 0$, iterate until convergence

$$\begin{cases} \text{1) Solve } \xi^k = \text{argmin}_{\xi\in Y} G(\mathcal{O}^k,\xi). \end{cases}$$

Bi-level formulation

Proposition

The mixed lightweight design composite problem can be equivalently written as

$$\min_{\mathcal{O}\in\mathcal{U}_{ad}} \{V(\mathcal{O})|\mathcal{M}(\mathcal{O}) \leq 0\},$$

where $\mathcal{M}$ constraint margin function $\mathcal{M}(\mathcal{O}) := \min_{\xi\in Y} G(\mathcal{O},\xi)$.

Optimization algorithm

Let $\mathcal{O}^0 \in \mathcal{U}_{ad}$ be an initial feasible point. For $k \geq 0$, iterate until convergence

$$\begin{cases} \text{1) Solve } \xi^k = \text{argmin}_{\xi\in Y} G(\mathcal{O}^k,\xi). \\ \text{2) Find } \mathcal{O}^{k+1} \text{ such that } V(\mathcal{O}^{k+1}) < V(\mathcal{O}^k) \text{ and } G(\mathcal{O}^{k+1},\xi^k) \leq 0. \end{cases}$$

Bi-level formulation

Proposition

The mixed lightweight design composite problem can be equivalently written as

$$\min_{\mathcal{O}\in\mathcal{U}_{ad}} \{V(\mathcal{O})|\mathcal{M}(\mathcal{O}) \leq 0\},$$

where $\mathcal{M}$ constraint margin function $\mathcal{M}(\mathcal{O}) := \min_{\xi\in Y} G(\mathcal{O},\xi)$.

Optimization algorithm

Let $\mathcal{O}^0 \in \mathcal{U}_{ad}$ be an initial feasible point. For $k \geq 0$, iterate until convergence

$$\begin{cases} \text{1) Solve } \xi^k = \text{argmin}_{\xi\in Y} G(\mathcal{O}^k,\xi). \\ \text{2) Find } \mathcal{O}^{k+1} \text{ such that } V(\mathcal{O}^{k+1}) < V(\mathcal{O}^k) \text{ and } G(\mathcal{O}^{k+1},\xi^k) \leq 0. \end{cases}$$

1) Integer programming solver 2) Level-set method.

Bi-level formulation

Proposition

The mixed lightweight design composite problem can be equivalently written as

$$\min_{\mathcal{O}\in\mathcal{U}_{ad}} \{V(\mathcal{O})|\mathcal{M}(\mathcal{O}) \leq 0\},$$

where $\mathcal{M}$ constraint margin function $\mathcal{M}(\mathcal{O}) := \min_{\xi\in Y} G(\mathcal{O},\xi)$.

Optimization algorithm

Let $\mathcal{O}^0 \in \mathcal{U}_{ad}$ be an initial feasible point. For $k \geq 0$, iterate until convergence

$$\begin{cases} \text{1) Solve } \xi^k = \text{argmin}_{\xi\in Y} G(\mathcal{O}^k,\xi). \\ \text{2) Find } \mathcal{O}^{k+1} \text{ such that } V(\mathcal{O}^{k+1}) < V(\mathcal{O}^k) \text{ and } G(\mathcal{O}^{k+1},\xi^k) \leq 0. \end{cases}$$

1) Integer programming solver 2) Level-set method.

Bi-level formulation

Proposition

The mixed lightweight design composite problem can be equivalently written as

$$\min_{\mathcal{O}\in\mathcal{U}_{ad}} \{V(\mathcal{O})|\mathcal{M}(\mathcal{O}) \leq 0\},$$

where $\mathcal{M}$ constraint margin function $\mathcal{M}(\mathcal{O}) := \min_{\xi\in Y} G(\mathcal{O},\xi)$.

Optimization algorithm

Let $\mathcal{O}^0 \in \mathcal{U}_{ad}$ be an initial feasible point. For $k \geq 0$, iterate until convergence

$$\begin{cases} \text{1) Solve } \xi^k = \text{argmin}_{\xi\in Y} G(\mathcal{O}^k,\xi). \\ \text{2) Find } \mathcal{O}^{k+1} \text{ such that } V(\mathcal{O}^{k+1}) < V(\mathcal{O}^k) \text{ and } G(\mathcal{O}^{k+1},\xi^k) \leq 0. \end{cases}$$

1) Integer programming solver 2) Level-set method.

Multi-phase shape sensitivity analysis

- Introduce the general criterion $J(\omega) = \int_\Omega j(x,u)\,dx$

Multi-phase shape sensitivity analysis

- Introduce the general criterion $J(\omega) = \int_\Omega j(x,u)\,dx$
- Some formulae of $J'(\omega)(\theta)$ in engineering literature are incorrect.

Multi-phase shape sensitivity analysis

- Introduce the general criterion $J(\omega) = \int_\Omega j(x,u)\,dx$
- Some formulae of $J'(\omega)(\theta)$ in engineering literature are incorrect.
- In a multi-phase framework, three shape derivative formulae arise:

Multi-phase shape sensitivity analysis

- Introduce the general criterion $J(\omega) = \int_\Omega j(x,u)\,dx$
- Some formulae of $J'(\omega)(\theta)$ in engineering literature are incorrect.
- In a multi-phase framework, three shape derivative formulae arise:

Proposition [Allaire, Dapogny, Delgado & Michailidis (2014)]
I. Continuous sharp interface

The shape derivative of J reads

$$J'(\omega)(\theta) = -\int_{\partial\omega} D(u,p)\,\theta\cdot n\,ds, \qquad \text{with}$$

$$D(u,p) = -\sigma(p)_{nn} : [\![e(u)_{nn}]\!] - 2\sigma(p)_{n\tau} : [\![e(u)_{n\tau}]\!] + [\![\sigma(u)_{\tau\tau}]\!] : e(p)_{\tau\tau}.$$

where $\sigma(v) = \mathcal{A}\,e(v)$ and p is the adjoint state, solution of

$$-\text{div}\,(\mathcal{A}e(p)) = -j'(x,u) \text{ in } \Omega, \quad \mathcal{A}e(p)\cdot n = 0 \text{ on } \Gamma_N, \quad p = 0 \text{ on } \Gamma_D.$$

Multi-phase shape sensitivity analysis

Proposition [Allaire, Dapogny, Delgado & Michailidis (2014)]

II. Discrete sharp interface

Let Ω_h be a conformal simplicial mesh of Ω and u_h, p_h the finite element approximations of u, p, respectively. Suppose that $\partial\omega$ is never aligned with the face of an element of Ω_h. Then the discrete shape derivative of $J_h(\omega) = \int_{\Omega_h} j(x, u_h)dx$ reads

$$J_h'(\omega)(\theta) = -\int_{\partial\omega} [\![\mathcal{A}]\!] e(u_h) : e(p_h)\, \theta \cdot n \, ds.$$

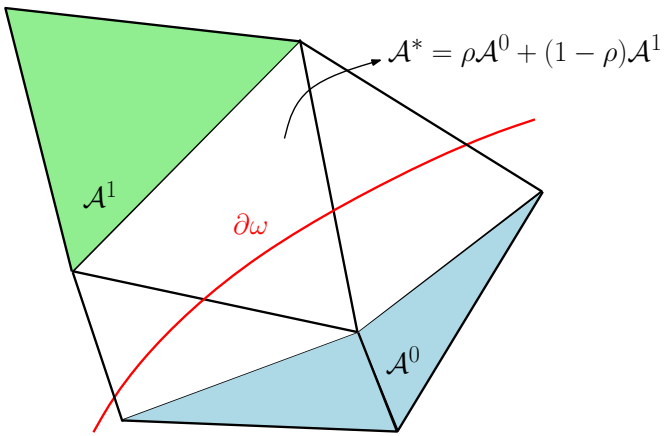

$$\sigma^0(u_h^0)\cdot n^0 \neq \sigma^1(u_h^1)\cdot n^1$$

$$u_h^0 = u_h^1$$

$$\mathcal{A}^* = \rho\mathcal{A}^0 + (1-\rho)\mathcal{A}^1$$

Multi-phase shape sensitivity analysis

Proposition [Allaire, Dapogny, Delgado & Michailidis (2014)]
III. Smooth interface

Consider the smooth interface frame $\mathcal{A} = \mathcal{A}^1 + H_\epsilon(d_\omega)(\mathcal{A}^0 - \mathcal{A}^1)$, with d_ω the signed distance function. Then the function J is shape differentiable in the sense of Gâteaux, and

$$J'_\epsilon(\Omega^0)(\theta) = -\int_{\partial\omega} \theta(x)\cdot n(x) \sum_{j=0}^{1} f_j(x)dx,$$

$$f_j(x) = \int_{\mathrm{ray}_{\partial\omega(x)}\cap\omega^j} H'_\varepsilon\left(d(z)\right)(\mathcal{A}^1 - \mathcal{A}^0)e(u)(z) : e(p)(z)(1 + d(z)\kappa)dz.$$

Multi-phase shape sensitivity analysis

Proposition [Allaire, Dapogny, Delgado & Michailidis (2014)]
III. Smooth interface

Consider the smooth interface frame $\mathcal{A} = \mathcal{A}^1 + H_\epsilon(d_\omega)(\mathcal{A}^0 - \mathcal{A}^1)$, with d_ω the signed distance function. Then the function J is shape differentiable in the sense of Gâteaux, and

$$J'_\epsilon(\Omega^0)(\theta) = -\int_{\partial\omega} \theta(x)\cdot n(x) \sum_{j=0}^{1} f_j(x)dx,$$

$$f_j(x) = \int_{\mathrm{ray}_{\partial\omega(x)}\cap\omega^j} H'_\varepsilon\left(d(z)\right)(\mathcal{A}^1 - \mathcal{A}^0)e(u)(z) : e(p)(z)(1 + d(z)\kappa)dz.$$

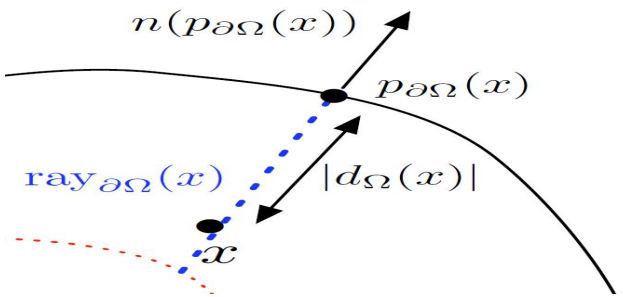

Multi-phase shape sensitivity analysis

Proposition [Allaire, Dapogny, Delgado & Michailidis (2014)]
III. Smooth interface

Consider the smooth interface frame $\mathcal{A} = \mathcal{A}^1 + H_\epsilon(d_\omega)(\mathcal{A}^0 - \mathcal{A}^1)$, with d_ω the signed distance function. Then the function J is shape differentiable in the sense of Gâteaux, and

$$J'_\epsilon(\Omega^0)(\theta) = -\int_{\partial\omega} \theta(x)\cdot n(x) \sum_{j=0}^{1} f_j(x)dx,$$

$$f_j(x) = \int_{\mathrm{ray}_{\partial\omega(x)}\cap\omega^j} H'_\varepsilon\left(d(z)\right)(\mathcal{A}^1 - \mathcal{A}^0)e(u)(z) : e(p)(z)(1 + d(z)\kappa)dz.$$

Proposition (Convergence)

$$\lim_{\epsilon\to 0} J'_\epsilon(\omega)(\theta) = J'(\omega)(\theta), \quad \forall\theta \in W^{1,\infty}(\Omega;\mathbb{R}^2)$$

Test case formulation: Composite fuselage skin panel

- $\Omega = \{x \in [0,2] \times [0,1]\}$. Symmetric multi-layered plate (16 plies).
- Each ply is composed of two phases (one of them "void").
- A shear load g is applied.

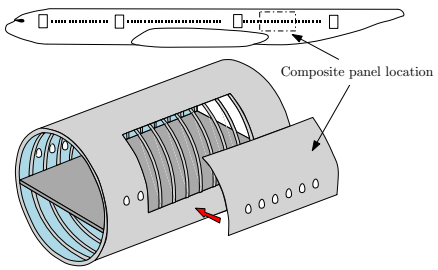

Figure: Approximative flat model.

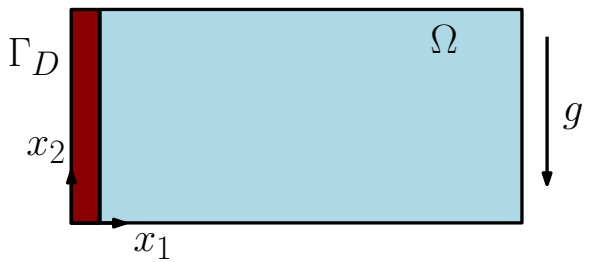

Figure: Composite test case.

Test case formulation: Composite fuselage skin panel

- $\Omega = \{x \in [0,2] \times [0,1]\}$. Symmetric multi-layered plate (16 plies).
- Each ply is composed of two phases (one of them "void").
- A shear load g is applied.

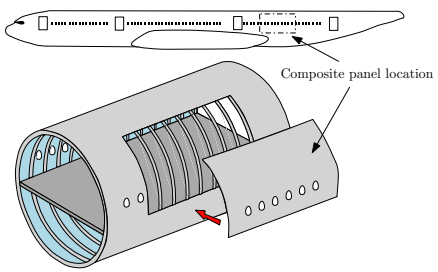

Figure: Approximative flat model.

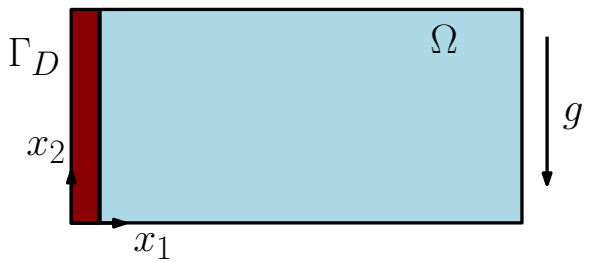

Figure: Composite test case.

- Optimization problem:

$$\min_{\mathcal{O} \in \mathcal{U}_{ad}, \xi \in Y} \left\{ \tilde{V}(\mathcal{O}) | \lambda_1^{-1}(\mathcal{O}, \xi) \leq 1 \right\},$$

Test case formulation: Composite fuselage skin panel

- $\Omega = \{x \in [0,2] \times [0,1]\}$. Symmetric multi-layered plate (16 plies).
- Each ply is composed of two phases (one of them "void").
- A shear load g is applied.

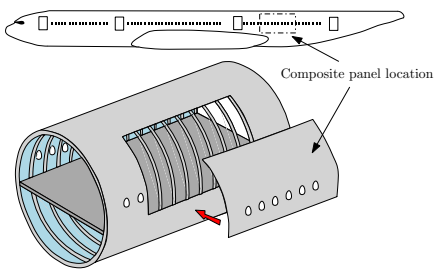

Figure: Approximative flat model.

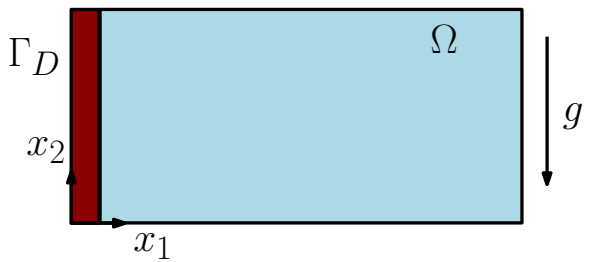

Figure: Composite test case.

- Optimization problem:

$$\min_{\mathcal{O}\in\mathcal{U}_{ad},\xi\in Y} \left\{ \tilde{V}(\mathcal{O}) | \lambda_1^{-1}(\mathcal{O},\xi) \leq 1 \right\}, \quad \tilde{V}(\mathcal{O}) = V(\mathcal{O}) + \gamma P(\mathcal{O}),\ \gamma > 0.$$

Test case formulation: Composite fuselage skin panel

- $\Omega = \{x \in [0,2] \times [0,1]\}$. Symmetric multi-layered plate (16 plies).
- Each ply is composed of two phases (one of them "void").
- A shear load g is applied.

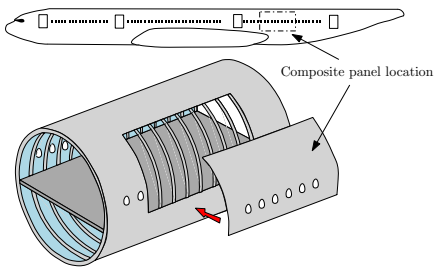

Figure: Approximative flat model.

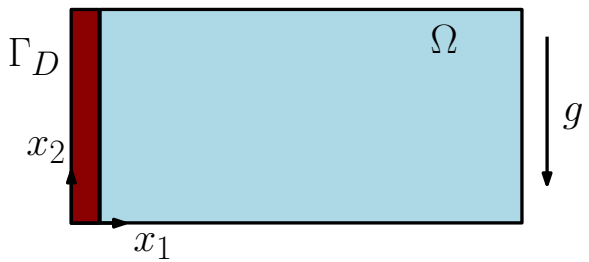

Figure: Composite test case.

- Optimization problem:

$$\min_{\mathcal{O}\in\mathcal{U}_{ad},\xi\in Y} \left\{ \tilde{V}(\mathcal{O}) | \lambda_1^{-1}(\mathcal{O},\xi) \leq 1 \right\}, \quad \tilde{V}(\mathcal{O}) = V(\mathcal{O}) + \gamma P(\mathcal{O}),\ \gamma > 0.$$

- Continuous algorithm: Sequential linear programming.
- Discrete algorithm: Outer approximation method.

Test case results

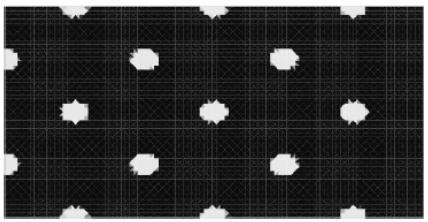

t0

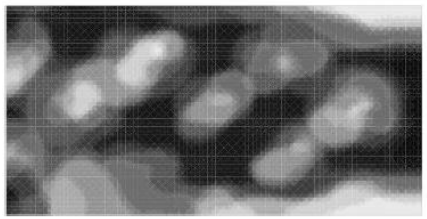

t1

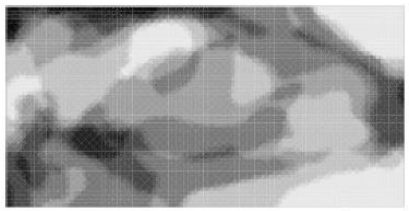

t2

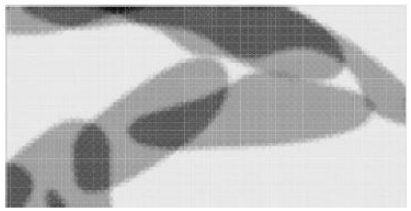

t3

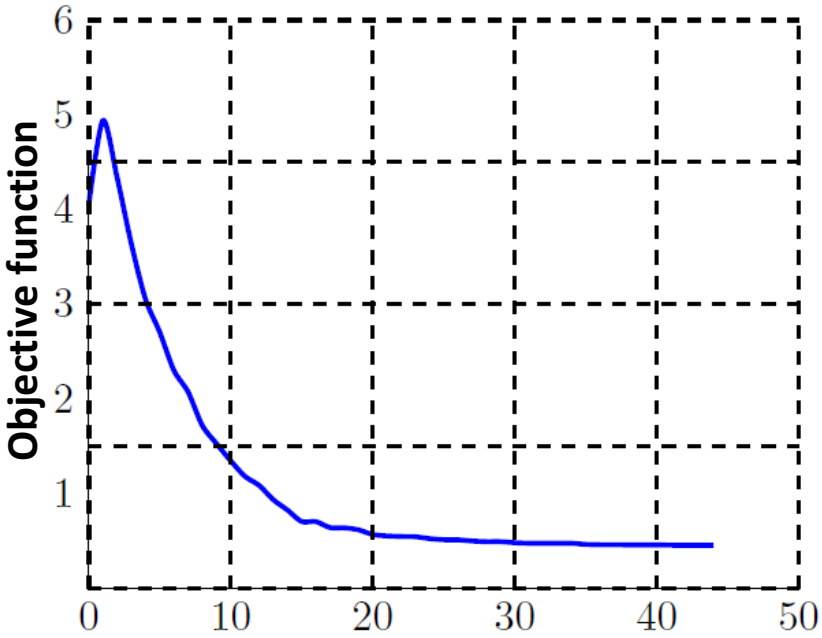

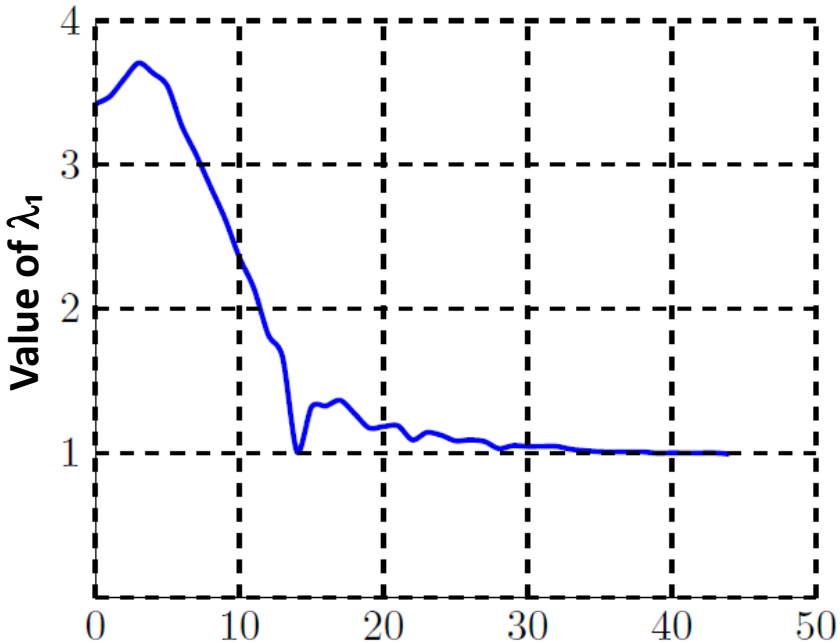

Test case results

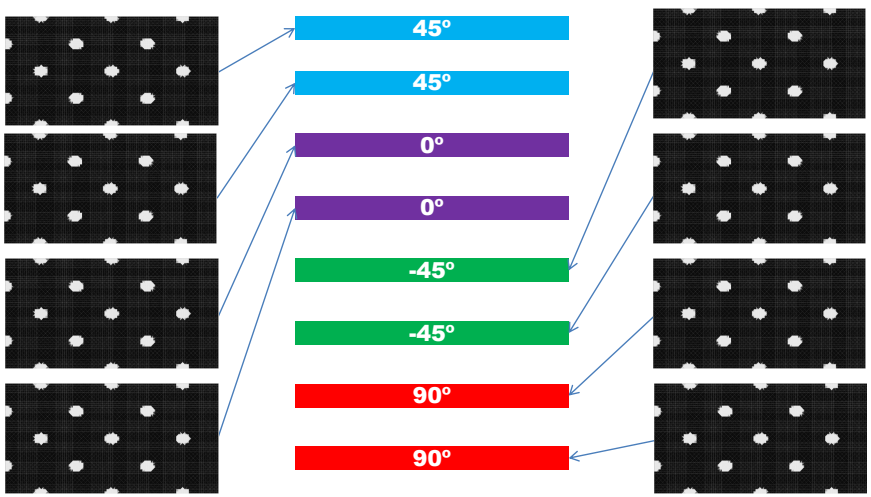

Figure: Initial configuration

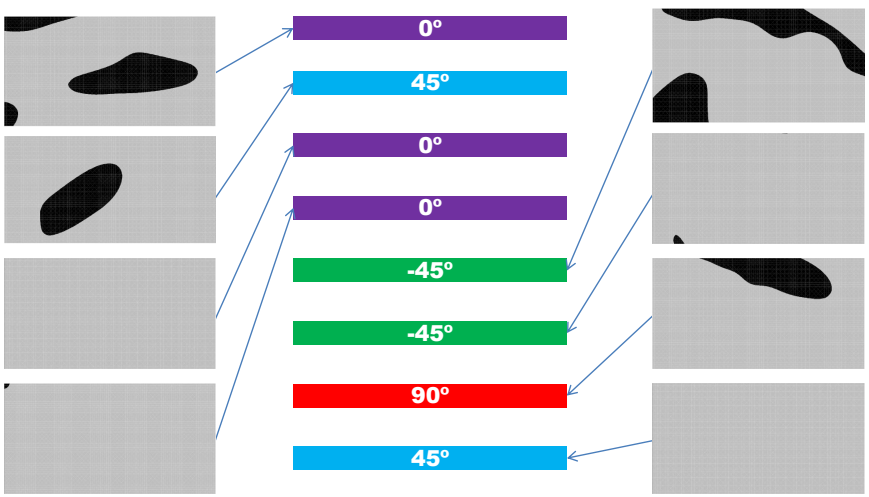

Figure: Final configuration (45 iter.)

Outline

Brief overview of the state of the art

Theory	*[Sokolowski & Zochowski99] *[Masmoudi98]

- Purpose: Measures the sensibility of a cost function J defined on $\Omega \subset \mathbb{R}^d$ w.r.t. the creation of a virtual inclusion B_a of size $a << 1$

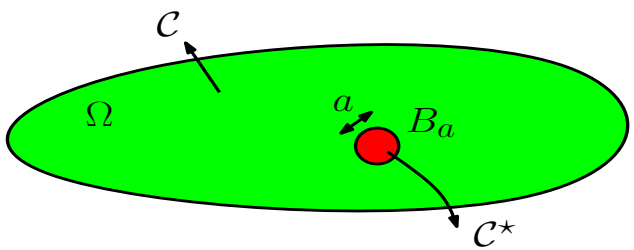

$$\begin{cases} \mathcal{C}: \text{ Physical properties } \Omega \\ \mathcal{C}^*: \text{ Physical properties } B_a \end{cases}$$

Brief overview of the state of the art

Theory	*[Sokolowski & Zochowski99] *[Masmoudi98]
Topology Optimization	*Bubble method [Schumacher, 1996] *Hard kill method [Nov02] *Level-set method [Ams04],[Alla05]
Inverse problems	*Flaw identification [Bon11],[Guz06] *Medical imaging [Ammari07]

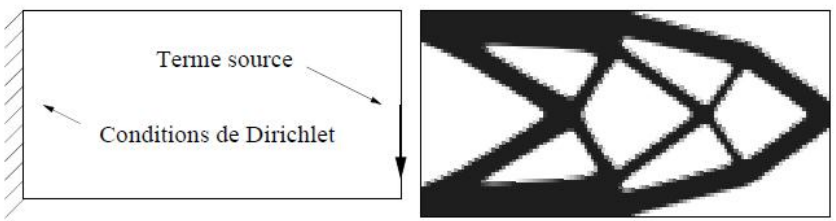

Figure: Topology Optimization

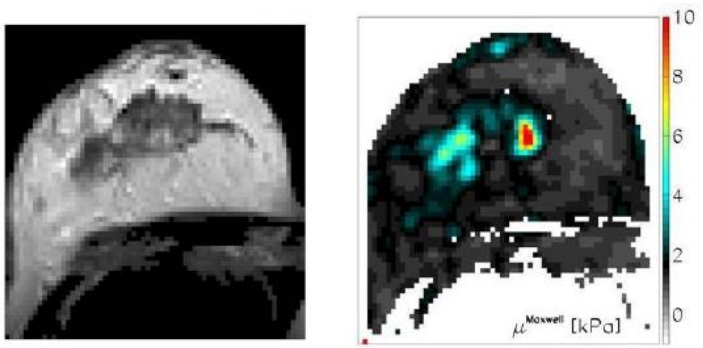

Figure: Inverse problems [Guz06]

Brief overview of the state of the art

Theory	*[Sokolowski & Zochowski99] *[Masmoudi98]
Topology Optimization	*Bubble method [Schumacher, 1996] *Hard kill method [Nov02] *Level-set method [Ams04],[Alla05]
Inverse problems	*Flaw identification [Bon11],[Guz06] *Medical imaging [Ammari07]

Criteria	*Energy functionals *Displacement-based functionals *Von-mises yield criterion

Brief overview of the state of the art

Theory	*[Sokolowski & Zochowski99] *[Masmoudi98]
Topology Optimization	*Bubble method [Schumacher, 1996] *Hard kill method [Nov02] *Level-set method [Ams04],[Alla05]
Inverse problems	*Flaw identification [Bon11],[Guz06] *Medical imaging [Ammari07]

Criteria	*Energy functionals *Displacement-based functionals *Von-mises yield criterion

Novelty of this work	*General anisotropic framework *Stress-based functionals

The topological derivative in 3D elastostatics

- Let u_a, u be the perturbed and non-perturbed elastic displacements within Ω.

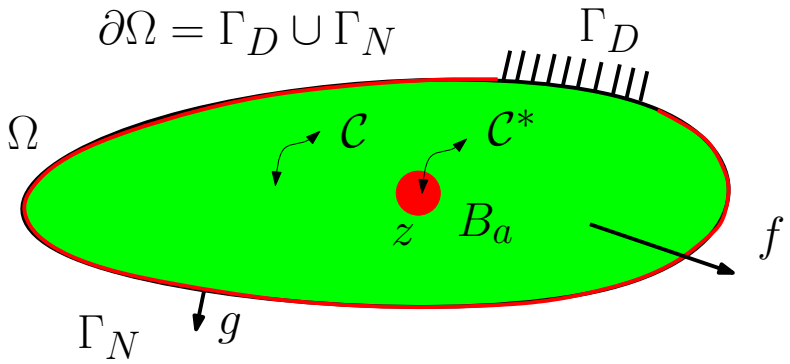

$$\begin{cases} \mathcal{C}: \text{ Elastic tensor in } \Omega \\ \mathcal{C}^*: \text{ Elastic tensor in } B_a \\ f, g: \text{ Volume \& Surface loads} \\ z: \text{ Center of } B_a \end{cases}$$

The topological derivative in 3D elastostatics

- Let u_a, u be the perturbed and non-perturbed elastic displacements within Ω.

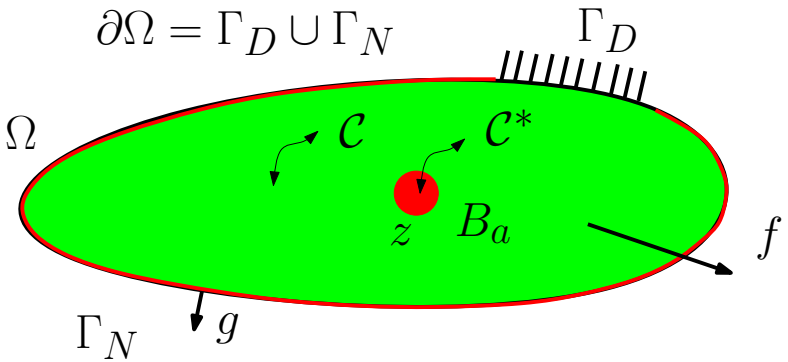

$$\begin{cases} \mathcal{C}: \text{ Elastic tensor in } \Omega \\ \mathcal{C}^*: \text{ Elastic tensor in } B_a \\ f, g: \text{ Volume \& Surface loads} \\ z: \text{ Center of } B_a \end{cases}$$

- where $W = \left\{ v \in H^1(\Omega; \mathbb{R}^3) | v = 0 \text{ on } \Gamma_D \subset \partial\Omega \right\}$ and $u_a, u \in W$ are solutions of:

$$\int_\Omega \nabla u : \mathcal{C}_a : \nabla v dx = \int_\Omega f \cdot v dx + \int_{\Gamma_N} g \cdot v ds, \quad \forall v \in W,$$

for $\mathcal{C}_a = \mathcal{C}^* \chi_{B_a} + \mathcal{C}(1 - \chi_{B_a})$ and $\mathcal{C}_0 = \mathcal{C}$, respectively.

The topological derivative in 3D elastostatics

- Let u_a, u be the perturbed and non-perturbed elastic displacements within Ω.
- The cost function will take the form

$$J(u_a, \nabla u_a) := \int_{\Omega \setminus B_a} \phi(x, u_a, \nabla u_a) dx + \int_{B_a} \phi^\star(x, u_a, \nabla u_a) dx$$

where $\phi, \phi^\star$ are twice differentiable and $\partial^2_{ij}\phi, \partial^2_{ij}\phi^\star \in C^{0,\alpha}$, $\alpha \in (0, 1)$.

The topological derivative in 3D elastostatics

- Let u_a, u be the perturbed and non-perturbed elastic displacements within Ω.
- The cost function will take the form

$$J(u_a, \nabla u_a) := \int_{\Omega \setminus B_a} \phi(x, u_a, \nabla u_a) dx + \int_{B_a} \phi^\star(x, u_a, \nabla u_a) dx$$

where $\phi, \phi^\star$ are twice differentiable and $\partial^2_{ij}\phi, \partial^2_{ij}\phi^\star \in C^{0,\alpha}$, $\alpha \in (0,1)$.

Definition

Let the cost functional J be and assume that it can be expanded in the form

$$J(u_a, \nabla u_a) - J(u, \nabla u) = a^3 DJ(z) + o(a^3).$$

Then $DJ(z)$ is called the topological derivative of J at $z \in \Omega$.

How to compute u_a for a small inhomogeneity?

Lemma

Consider the auxiliary problem of an inhomogeneity $(\mathcal{B},\ \mathcal{C}^\star)$ centered at the origin, embedded in an infinite elastic medium $(\mathbb{R}^3, \mathcal{C})$ subjected to an uniform remote strain $\nabla u(z), z \in \Omega$.

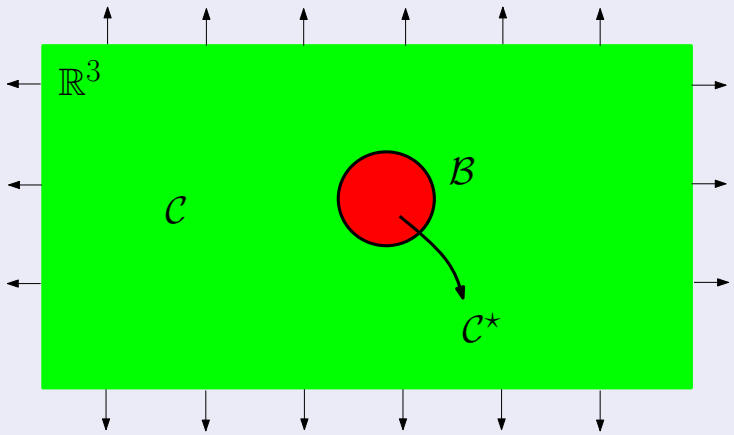

$$\begin{cases} u_{\mathcal{B}}: \text{ perturbed displacement in } \mathbb{R}^3 \\ u^\infty: \text{ unperturbed displacement in } \mathbb{R}^3 \\ u^\infty = \nabla u(z) \cdot x, x \in \mathbb{R}^3 \end{cases}$$

Suppose that $B_a = z + a\mathcal{B}$, then the following near-field development stands

$$u_a = u + a(u_{\mathcal{B}} - u^\infty)\left(\frac{x-z}{a}\right) + o(a).$$

Elastic moment tensor (EMT)

- More generally known as Polarization tensor [Nazarov, 2009].

Elastic moment tensor (EMT)

- More generally known as Polarization tensor [Nazarov, 2009].
- Depends on the geometry $\mathcal{B}$ and the elastic law $\mathcal{C}^*$ of an inclusion embedded in an elastic medium $\mathcal{C}$.

Elastic moment tensor (EMT)

- More generally known as Polarization tensor [Nazarov, 2009].
- Depends on the geometry $\mathcal{B}$ and the elastic law $\mathcal{C}^*$ of an inclusion embedded in an elastic medium $\mathcal{C}$.
- Important ingredient in the computation of the topological derivative.

Elastic moment tensor (EMT)

- More generally known as Polarization tensor [Nazarov, 2009].
- Depends on the geometry $\mathcal{B}$ and the elastic law $\mathcal{C}^*$ of an inclusion embedded in an elastic medium $\mathcal{C}$.
- Important ingredient in the computation of the topological derivative.

Definition

Let $u_{\mathcal{B}}$ denote the perturbed solution of the free-space transmission problem. The elastic moment tensor (EMT) $\mathcal{E}$ is defined for any value of $\nabla u(z)$ as

$$\mathcal{E} : \nabla u(z) = \int_{\mathcal{B}} (\mathcal{C}^\star - \mathcal{C}) : \nabla u_{\mathcal{B}} dx.$$

Main result

Proposition [Delgado and Bonnet, 2014 (review)]

Suppose $\mathcal{B}$ is an ellipsoid. The topological derivative at z of $J(u_a, \nabla u_a)$ reads

Main result

Proposition [Delgado and Bonnet, 2014 (review)]

Suppose $\mathcal{B}$ is an ellipsoid. The topological derivative at z of $J(u_a, \nabla u_a)$ reads

$$DJ(z) = -\nabla p(z) : \mathcal{E} : \nabla u(z) + |\mathcal{B}|(\phi^* - \phi)(z, u(z), \nabla u(z))$$
$$+ \partial_d(\phi^* - \phi)(z, u(z), \nabla u(z)) : \int_{\mathcal{B}} \nabla v_{\mathcal{B}}(x) dx$$
$$+ \int_{\mathbb{R}^3 \setminus \mathcal{B}} \mathcal{G}(z, \nabla v_{\mathcal{B}}(x)) dx + \int_{\mathcal{B}} \mathcal{G}^\star(z, \nabla v_{\mathcal{B}}(x)) dx.$$

Main result

Proposition [Delgado and Bonnet, 2014 (review)]

Suppose $\mathcal{B}$ is an ellipsoid. The topological derivative at z of $J(u_a, \nabla u_a)$ reads

$$DJ(z) = -\nabla p(z) : \mathcal{E} : \nabla u(z) + |\mathcal{B}|(\phi^* - \phi)(z, u(z), \nabla u(z))$$
$$+ \partial_d(\phi^* - \phi)(z, u(z), \nabla u(z)) : \int_{\mathcal{B}} \nabla v_{\mathcal{B}}(x) dx$$
$$+ \int_{\mathbb{R}^3 \setminus \mathcal{B}} \mathcal{G}(z, \nabla v_{\mathcal{B}}(x)) dx + \int_{\mathcal{B}} \mathcal{G}^\star(z, \nabla v_{\mathcal{B}}(x)) dx.$$

- The function $p \in W$ is the adjoint state.

Main result

Proposition [Delgado and Bonnet, 2014 (review)]

Suppose $\mathcal{B}$ is an ellipsoid. The topological derivative at z of $J(u_a, \nabla u_a)$ reads

$$DJ(z) = -\nabla p(z) : \mathcal{E} : \nabla u(z) + |\mathcal{B}|(\phi^* - \phi)(z, u(z), \nabla u(z))$$
$$+ \partial_d(\phi^* - \phi)(z, u(z), \nabla u(z)) : \int_{\mathcal{B}} \nabla v_{\mathcal{B}}(x) dx$$
$$+ \int_{\mathbb{R}^3 \setminus \mathcal{B}} \mathcal{G}(z, \nabla v_{\mathcal{B}}(x)) dx + \int_{\mathcal{B}} \mathcal{G}^\star(z, \nabla v_{\mathcal{B}}(x)) dx.$$

- The function $p \in W$ is the adjoint state.
- $v_{\mathcal{B}} = u_{\mathcal{B}} - u^\infty$ represents the free-space perturbation.

Main result

Proposition [Delgado and Bonnet, 2014 (review)]

Suppose $\mathcal{B}$ is an ellipsoid. The topological derivative at z of $J(u_a, \nabla u_a)$ reads

$$DJ(z) = -\nabla p(z) : \mathcal{E} : \nabla u(z) + |\mathcal{B}|(\phi^* - \phi)(z, u(z), \nabla u(z))$$
$$+ \partial_d(\phi^* - \phi)(z, u(z), \nabla u(z)) : \int_{\mathcal{B}} \nabla v_{\mathcal{B}}(x) dx$$
$$+ \int_{\mathbb{R}^3 \setminus \mathcal{B}} \mathcal{G}(z, \nabla v_{\mathcal{B}}(x)) dx + \int_{\mathcal{B}} \mathcal{G}^\star(z, \nabla v_{\mathcal{B}}(x)) dx.$$

- The function $p \in W$ is the adjoint state.
- $v_{\mathcal{B}} = u_{\mathcal{B}} - u^\infty$ represents the free-space perturbation.
- The function $\mathcal{G}(z, d)$ (respectively $\mathcal{G}^*(z, d)$) is defined as

$$\phi(z, u(z), \nabla u(z) + d) - \phi(z, u(z), \nabla u(z)) - \partial_d \phi(z, u(z), \nabla u(z)) : d$$

Main result

Proposition [Delgado and Bonnet, 2014 (review)]

Suppose $\mathcal{B}$ is an ellipsoid. The topological derivative at z of $J(u_a, \nabla u_a)$ reads

$$DJ(z) = -\nabla p(z) : \mathcal{E} : \nabla u(z) + |\mathcal{B}|(\phi^* - \phi)(z, u(z), \nabla u(z))$$
$$+ \partial_d(\phi^* - \phi)(z, u(z), \nabla u(z)) : \int_{\mathcal{B}} \nabla v_{\mathcal{B}}(x) dx$$
$$+ \int_{\mathbb{R}^3 \setminus \mathcal{B}} \mathcal{G}(z, \nabla v_{\mathcal{B}}(x)) dx + \int_{\mathcal{B}} \mathcal{G}^\star(z, \nabla v_{\mathcal{B}}(x)) dx.$$

- The function $p \in W$ is the adjoint state.
- $v_{\mathcal{B}} = u_{\mathcal{B}} - u^\infty$ represents the free-space perturbation.
- The function $\mathcal{G}(z, d)$ (respectively $\mathcal{G}^*(z, d)$) is defined as

$$\phi(z, u(z), \nabla u(z) + d) - \phi(z, u(z), \nabla u(z)) - \partial_d \phi(z, u(z), \nabla u(z)) : d$$

- Similar results: [Amstutz et al., 2012], [Schneider and Andrä, 2013].

Main result: remarks

- The choice of $\mathcal{B}$ as an ellipsoid allow us to use the following result [Eshelby, 1957]

$$\nabla v_{\mathcal{B}} = Cst, \quad \text{inside } \mathcal{B}$$

Main result: remarks

- The choice of $\mathcal{B}$ as an ellipsoid allow us to use the following result [Eshelby, 1957]

$$\nabla v_{\mathcal{B}} = Cst, \quad \text{inside } \mathcal{B}$$

- The computation of the EMT the follows as

$$\mathcal{E} = |\mathcal{B}|\mathcal{C} : (\mathcal{C} + \Delta\mathcal{C} : \mathcal{S})^{-1} : \Delta\mathcal{C}; \quad \mathcal{S} = \mathcal{S}(\mathcal{C}, \mathcal{B}) : \text{Eshelby tensor.}$$

Main result: remarks

- The choice of $\mathcal{B}$ as an ellipsoid allow us to use the following result [Eshelby, 1957]

$$\nabla v_{\mathcal{B}} = Cst, \quad \text{inside } \mathcal{B}$$

- The computation of the EMT the follows as

$$\mathcal{E} = |\mathcal{B}|\mathcal{C} : (\mathcal{C} + \Delta\mathcal{C} : \mathcal{S})^{-1} : \Delta\mathcal{C}; \quad \mathcal{S} = \mathcal{S}(\mathcal{C}, \mathcal{B}) : \text{Eshelby tensor.}$$

- New terms appearing in DJ are due to the dependence of J on ∇u_a.

Main result: remarks

- The choice of $\mathcal{B}$ as an ellipsoid allow us to use the following result [Eshelby, 1957]

$$\nabla v_{\mathcal{B}} = Cst, \quad \text{inside } \mathcal{B}$$

- The computation of the EMT the follows as

$$\mathcal{E} = |\mathcal{B}|\mathcal{C} : (\mathcal{C} + \Delta\mathcal{C} : \mathcal{S})^{-1} : \Delta\mathcal{C}; \quad \mathcal{S} = \mathcal{S}(\mathcal{C}, \mathcal{B}) : \text{Eshelby tensor.}$$

- New terms appearing in DJ are due to the dependence of J on ∇u_a.
- In particular the evaluation of the term

$$\int_{\mathbb{R}^3 \setminus \mathcal{B}} \mathcal{G}(z, \nabla v_{\mathcal{B}}(x)) dx$$

is numerically expensive to integrate.

Numerical applications in non-destructive control

- Objective: Detection of an elastic default or anomaly in an anisotropic medium.

Numerical applications in non-destructive control

- Objective: Detection of an elastic default or anomaly in an anisotropic medium.
- Cost functional: Full-field kinematical measurements over a set of control volumes $\omega \subset \Omega$

$$J(\nabla u_a) = \int_\omega \nabla(u_a - u^*) : \mathcal{C}_a : \nabla(u_a - u^*) dx.$$

Numerical applications in non-destructive control

- Objective: Detection of an elastic default or anomaly in an anisotropic medium.
- Cost functional: Full-field kinematical measurements over a set of control volumes $\omega \subset \Omega$

$$J(\nabla u_a) = \int_\omega \nabla(u_a - u^*) : \mathcal{C}_a : \nabla(u_a - u^*) dx.$$

- u_a is the virtual perturbed displacement.

Numerical applications in non-destructive control

- Objective: Detection of an elastic default or anomaly in an anisotropic medium.
- Cost functional: Full-field kinematical measurements over a set of control volumes $\omega \subset \Omega$

$$J(\nabla u_a) = \int_\omega \nabla(u_a - u^*) : \mathcal{C}_a : \nabla(u_a - u^*) dx.$$

- u_a is the virtual perturbed displacement.
- u^* corresponds to the measured data.

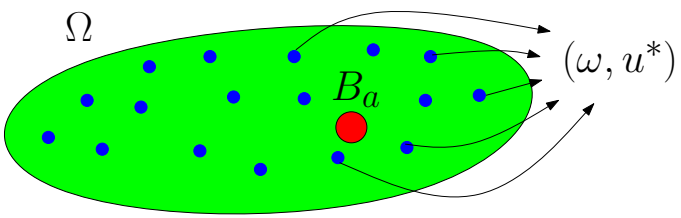

Figure: Full-field measurement setting

Numerical applications in non-destructive control

- Objective: Detection of an elastic default or anomaly in an anisotropic medium.
- Cost functional: Full-field kinematical measurements over a set of control volumes $\omega \subset \Omega$

$$J(\nabla u_a) = \int_\omega \nabla(u_a - u^*) : \mathcal{C}_a : \nabla(u_a - u^*) dx.$$

- u_a is the virtual perturbed displacement.
- u^* corresponds to the measured data.

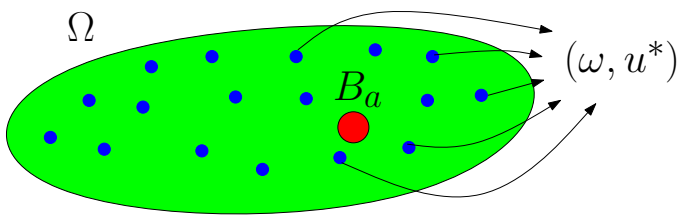

Figure: Full-field measurement setting

- Some examples: Magnetic resonance elastography [Yuan et al., 2012], Digital image correlation via X-ray tomography [Bay et al., 1999].

Numerical applications in non-destructive control

- Let $z \in \Omega$. Suppose that either a) $\omega = \Omega$ or b) $z \notin \omega$:

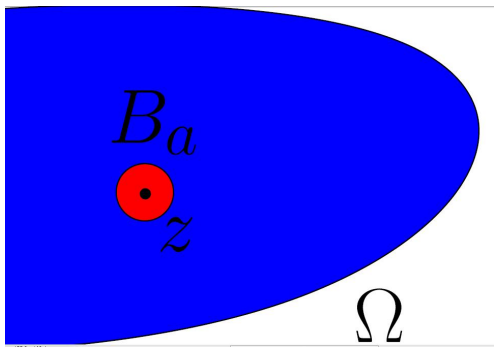

Figure: $\omega = \Omega$

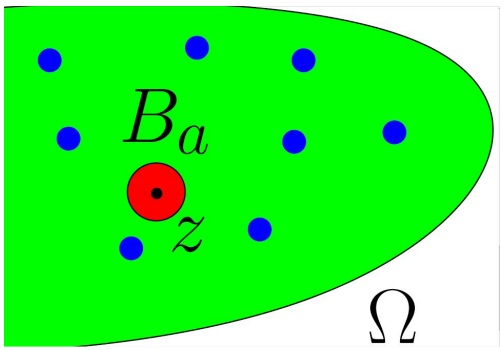

Figure: $z \notin \omega$

Numerical applications in non-destructive control

- Let $z \in \Omega$. Suppose that either a) $\omega = \Omega$ or b) $z \notin \omega$:

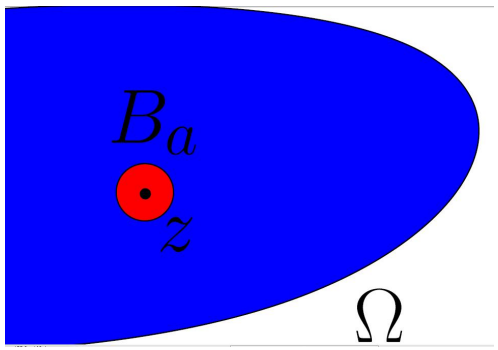

Figure: $\omega = \Omega$

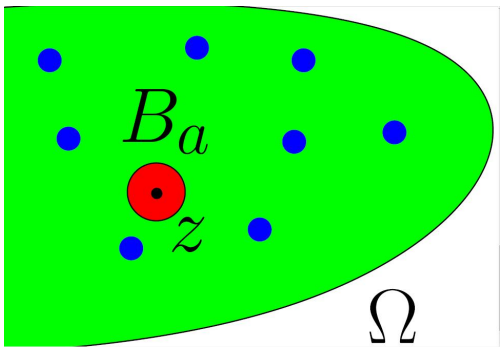

Figure: $z \notin \omega$

- Then the topological derivative formula simplifies

$$DJ(z) = -\nabla p(z) : \mathcal{E} : \nabla u(z)$$

Numerical applications in non-destructive control

- Let $z \in \Omega$. Suppose that either a) $\omega = \Omega$ or b) $z \notin \omega$:

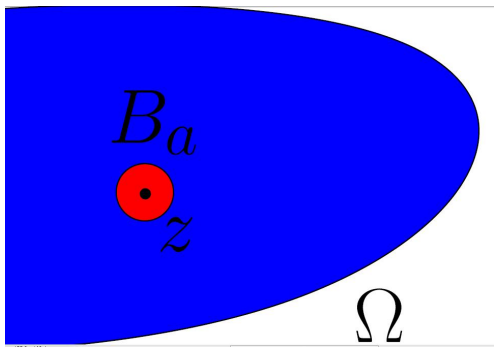

Figure: $\omega = \Omega$

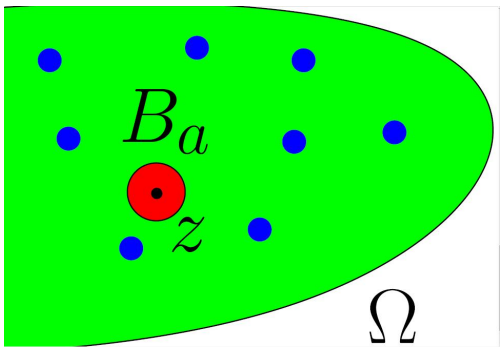

Figure: $z \notin \omega$

- Then the topological derivative formula simplifies

$$DJ(z) = -\nabla p(z) : \mathcal{E} : \nabla u(z)$$

- The goal is to find the places z where DJ attains the most negative values.

First application: 2D framework, $\omega = \Omega$

- Objective: Identify each inclusion.

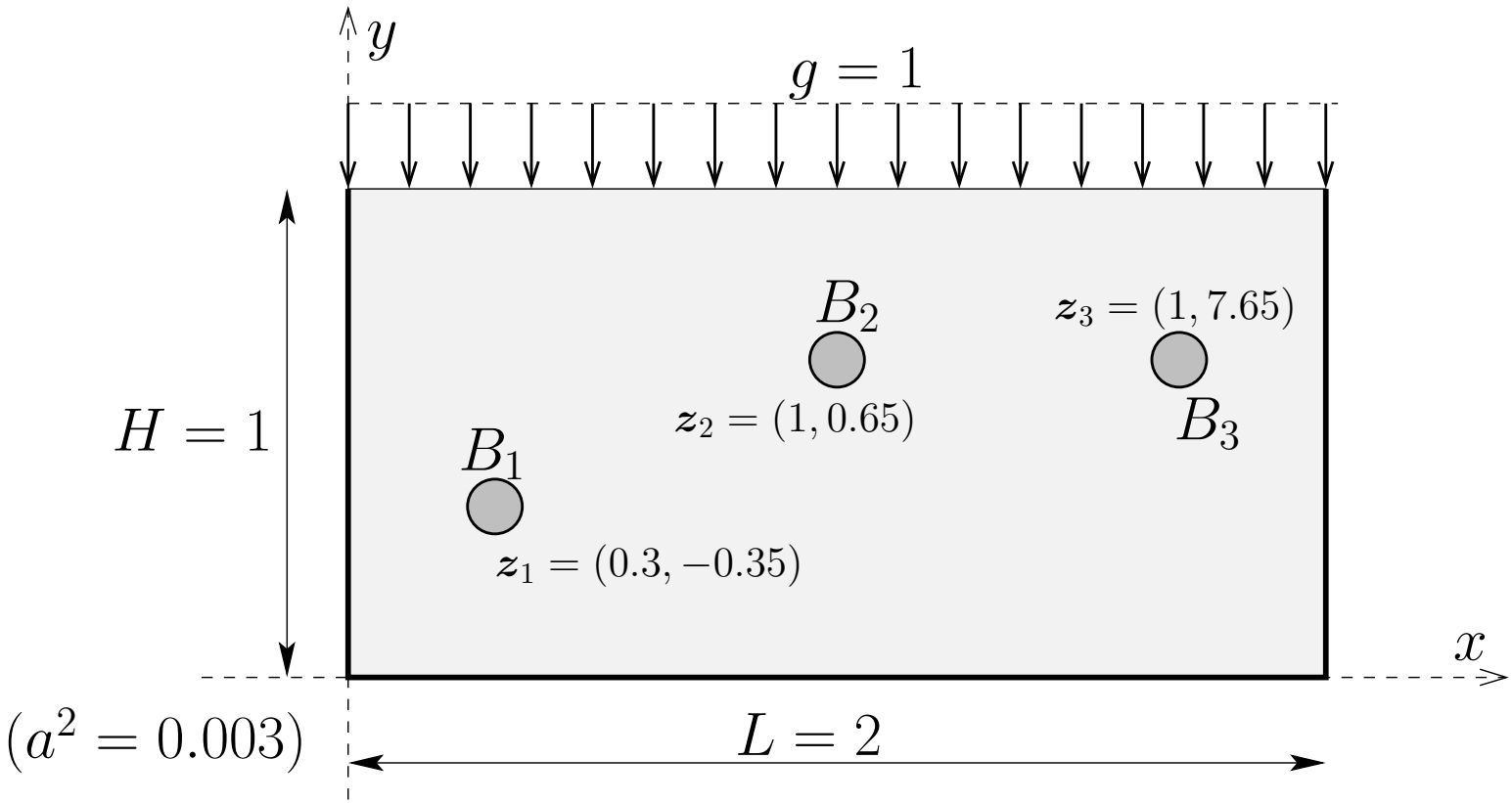

Figure: Orthotropic medium $\mathcal{C}$ ($E_1 = 0.1, E_2 = 1, \nu_{12} = 0.3, G_{12} = 0.03$) with three inclusions: B_1, B_3 are softer ($\mathcal{C}^* = 0.5\mathcal{C}$) while B_2 is harder ($\mathcal{C}^* = 2\mathcal{C}$).

First application: Results

Figure: Values of DJ using as test material $\mathcal{C}^* = 0.5\mathcal{C}$.

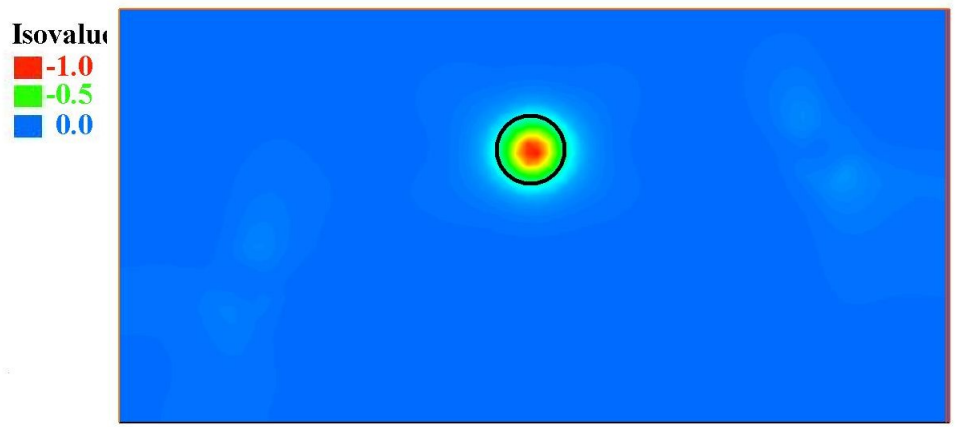

Figure: Values of DJ using as test material $\mathcal{C}^* = 2\mathcal{C}$.

Second application: 3D composite framework, $\omega \subset \Omega$

- Objective: Detect the failure point

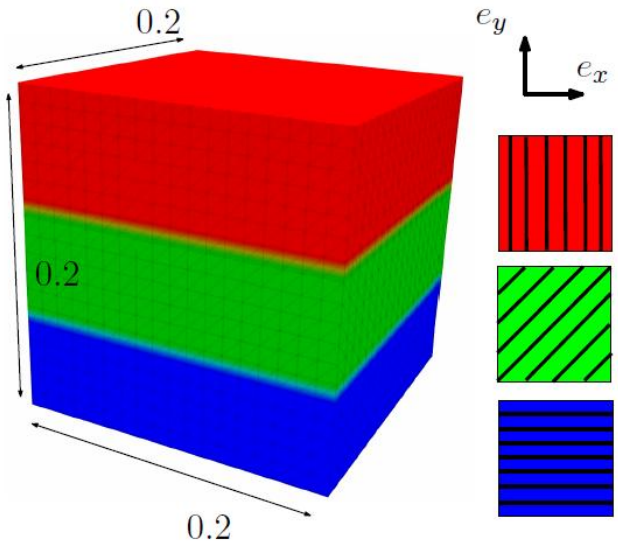

Figure: Multi-layered cube made of three orthotropic materials $\mathcal{C}_1, \mathcal{C}_2, \mathcal{C}_3$. Failure point $\mathcal{C}^* = 10^{-5} \times \mathcal{C}$

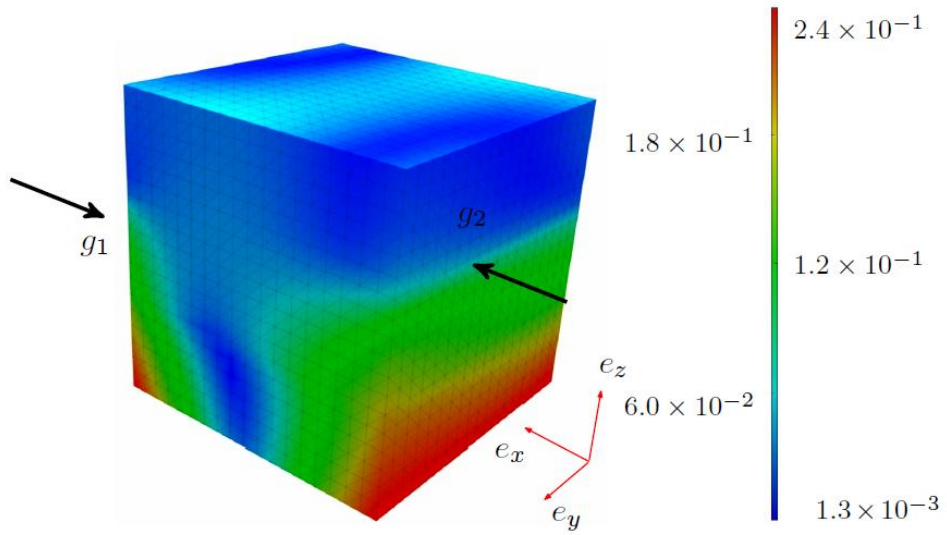

Figure: Elastic displacements after the application of the loads g_1, g_2.

Second application: Results

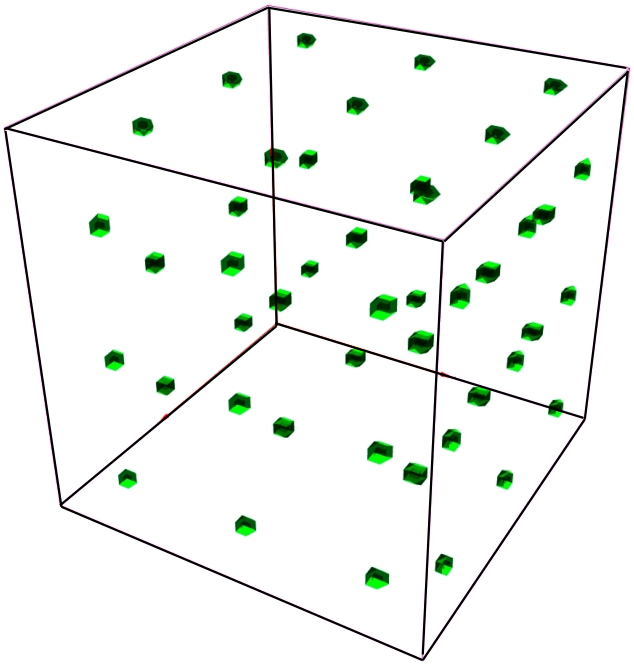

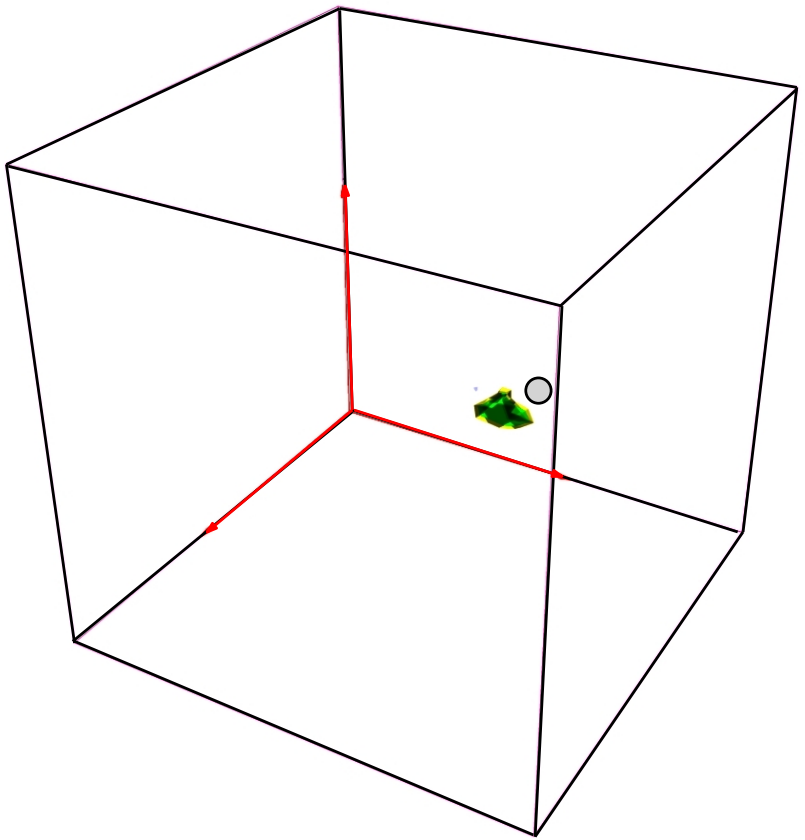

Figure: $\omega = \cup\{\omega_i\}_{i=1,\ldots,44}$.

Green: DJ iso-surfaces around its minimum value -1.3×10^{-3}.

Gray: Show the correct location of the failure point.

Second application: Results

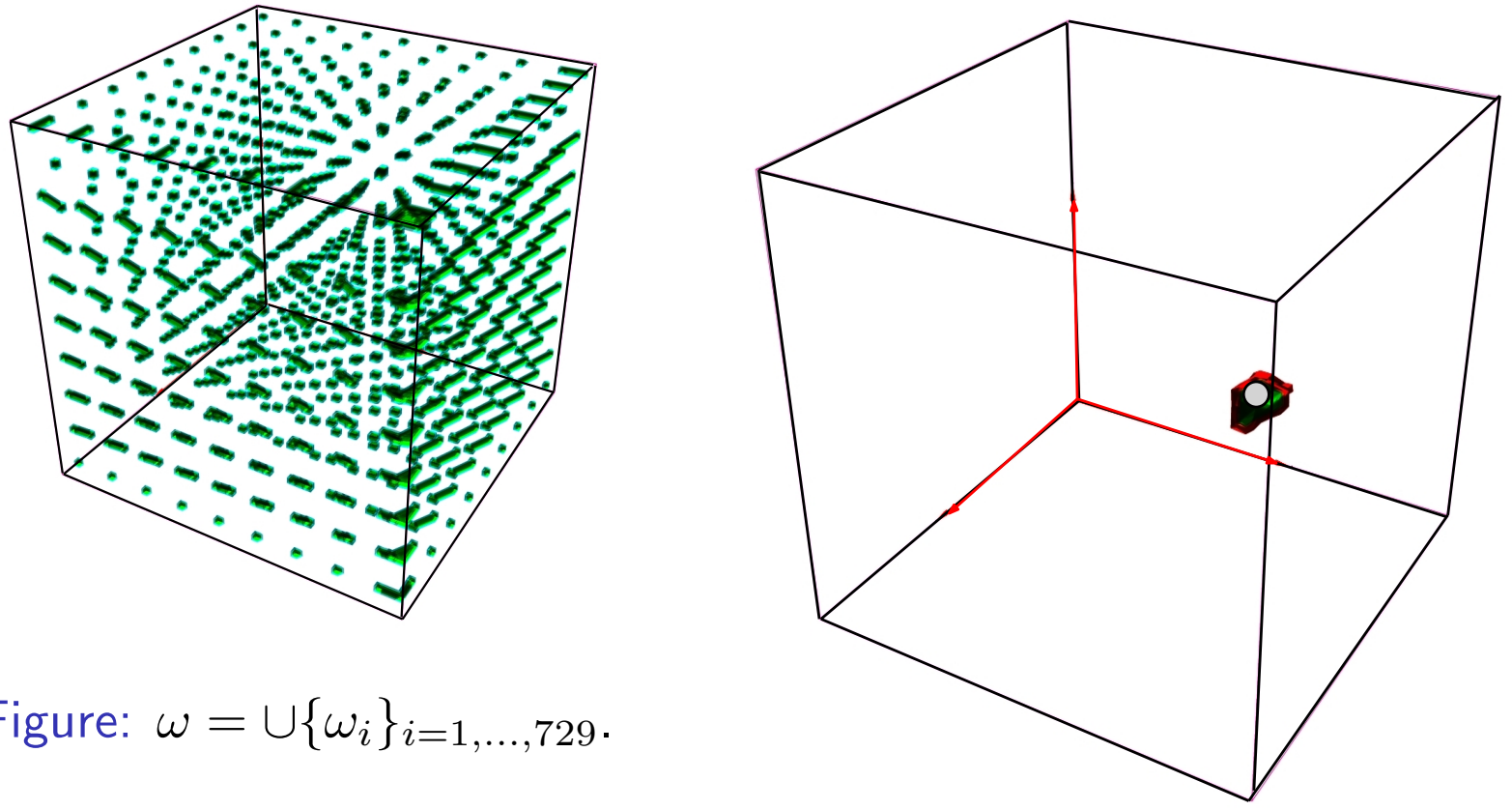

Figure: $\omega = \cup\{\omega_i\}_{i=1,\ldots,729}$.

Green: DJ iso-surfaces around its minimum value -6.9×10^{-2}.
Gray: Show the correct location of the failure point.

Outline

Conclusions

- This thesis was set as an exploratory work to ameliorate composite design in industry via the level-set technology.

Conclusions

- This thesis was set as an exploratory work to ameliorate composite design in industry via the level-set technology.
- The level-set method was extended to a multi-phase & multi-layered composite framework.

Conclusions

- This thesis was set as an exploratory work to ameliorate composite design in industry via the level-set technology.
- The level-set method was extended to a multi-phase & multi-layered composite framework.
- Various approximations of the shape derivative (sharp, smeared & discrete) were given in an anisotropic multi-phase framework.

Conclusions

- This thesis was set as an exploratory work to ameliorate composite design in industry via the level-set technology.
- The level-set method was extended to a multi-phase & multi-layered composite framework.
- Various approximations of the shape derivative (sharp, smeared & discrete) were given in an anisotropic multi-phase framework.
- The topological derivative for anisotropic materials was studied for a large class of criteria.

Perspectives

- Enrich the composite problem with a more realistic shell model & other manufacturing constraints for industrial applications.

Perspectives

- Enrich the composite problem with a more realistic shell model & other manufacturing constraints for industrial applications.

- Introduce the topological derivative in the topology optimization loop of the level-set algorithm.

Perspectives

- Enrich the composite problem with a more realistic shell model & other manufacturing constraints for industrial applications.
- Introduce the topological derivative in the topology optimization loop of the level-set algorithm.
- Perform a robustness and sensitivity analysis of the topological derivative for non-destructive control.

Perspectives

- Enrich the composite problem with a more realistic shell model & other manufacturing constraints for industrial applications.
- Introduce the topological derivative in the topology optimization loop of the level-set algorithm.
- Perform a robustness and sensitivity analysis of the topological derivative for non-destructive control.
- Extend the computation of the topological derivative to an elastodynamic framework.

Thank you for your attention!

Communications

- G. Allaire, C. Dapogny, G. Delgado, and G. Michailidis. *Mutli-phase structural optimization via a level-set method*. ESAIM: Control, Optimisation and Calculus of Variations (2014).
- M. Bonnet, G. Delgado. *The topological derivative in anisotropic elasticity*. Quarterly Journal of Mechanics and Applied Mathematics (2013).
- G. Delgado, M. Bonnet. *The topological derivative of stress-based cost functionals in anisotropic elasticity*. Submitted (2014).
- G. Allaire, G. Delgado. *Stacking sequence and shape optimization of laminated composite plates via a level-set method*. In preparation (2014).

References I

G. Allaire, F. Jouve, and A.M. Toader. A level-set method for shape optimization. *Comptes Rendus Mathematique*, 334(12):1125–1130, 2002.

S Amstutz, A. A. Novotny, and E. A. de Souza Neto. Topological derivative-based topology optimization of structures subject to drucker-prager stress constraints. *Comp. Meth. Appl. Mech. Eng.*, 233: 123–136, 2012.

Brian K Bay, Tait S Smith, David P Fyhrie, and Malik Saad. Digital volume correlation: three-dimensional strain mapping using x-ray tomography. *Experimental Mechanics*, 39(3):217–226, 1999.

Martin Philip Bendsøe. *Optimization of structural topology, shape, and material*. Springer, 1995.

References II

M.P. Bendsøe and N. Kikuchi. Generating optimal topologies in structural design using a homogenization method. *Computer methods in applied mechanics and engineering*, 71(2):197–224, 1988.

A Chambolle and B Bourdin. Optimisation topologique de structures soumises à des forces de pression. *Actes du 32ème Congrès National d'Analyse Numérique.*, 2000.

J. D. Eshelby. The determination of the elastic field of an ellipsoidal inclusion and related problems. *Proc. Roy. Soc. A*, 241:376–396, 1957.

Jacques Hadamard. *Mémoire sur le problème d'analyse relatif à l'équilibre des plaques élastiques encastrées*, volume 33. Imprimerie nationale, 1908.

François Murat and Luc Tartar. Calcul des variations et homogénéisation, In les méthodes de l'homogénéisation: théorie et applications en physique. *Coll. Dir. Etudes et Recherches EDF*, (57):319–369, 1985.

References III

SA Nazarov. Elasticity polarization tensor, surface enthalpy, and eshelby theorem. *Journal of Mathematical Sciences*, 159(2):133–167, 2009.

S. Osher and J.A. Sethian. Fronts propagating with curvature-dependent speed: algorithms based on hamilton-jacobi formulations. *Journal of computational physics*, 79(1):12–49, 1988.

Axel Schumacher. *Topologieoptimierung von Bauteilstrukturen unter Verwendung von Lochpositionierungskriterien*. PhD thesis, Forschungszentrum für Multidisziplinäre Analysen und Angewandte Strukturoptimierung. Institut für Mechanik und Regelungstechnik, 1996.

J. Simon and F. Murat. Sur le contrôle par un domaine géométrique. *Publication 76015 du Laboratoire d'Analyse Numérique de l'Université Paris VI*, (76015):222 pages, 1976.

References IV

M.Y. Wang, X. Wang, and D. Guo. A level set method for structural topology optimization. *Computer methods in applied mechanics and engineering*, 192(1):227–246, 2003.

H. Yuan, B. B. Guzina, and R. Sinkus. Application of topological sensitivity toward tissue elasticity imaging using magnetic resonance data. *J. Eng. Mech. ASCE*, 2012.